FLOW FIELD AND SCOURING EFFECTS OF STEADY AND PULSATING JETS IMPINGING ON A MOVABLE BED

(Abschlußbericht B 2)

von

H. Kobus, P. Leister und B. Westrich

SFB 80/ET/92
März 1977

SONDERFORSCHUNGSBEREICH 80
AUSBREITUNGS- UND TRANSPORTVORGÄNGE IN STRÖMUNGEN
U N I V E R S I T Ä T K A R L S R U H E

INHALTSVERZEICHNIS

TEIL A

TÄTIGKEITSBERICHT ZUM TEILPROJEKT B 2

"Einfluß stationärer und pulsierender Strahlen
auf die Erosion eines Sandbettes"

1. Übersicht

Das Teilprojekt B 2 wurde in den Jahren 1970 - 1977 am Institut für Hydromechanik unter der Leitung von H. Kobus bearbeitet und in der Zeit vom 1.4.1970 - 30.6.1975 vom Sonderforschungsbereich 80 finanziell gefördert. Als wissenschaftliche Mitarbeiter waren die Herren B. Westrich in den Jahren 1970 - 1974 und P. Leister in den Jahren 1973 - 1977 an diesem Projekt tätig. Weiterhin wirkten als technische Mitarbeiter die Herren D. Danzeisen, Betriebsingenieur (1971 - 1977), W. Fuchs, Techniker (1972), H. Beran, Techniker (1974/75) sowie R. Fink, Laborant (1971/72) an den experimentellen Arbeiten zu diesem Projekt mit.

Im Rahmen des Forschungsvorhabens entstanden zwei Promotionen. Herr B. Westrich schloß im Jahr 1974 den ersten Teil des Untersuchungsprogramms am Wassermodell mit seiner Promotion ab, und Herr P. Leister führte die Arbeiten am Luftmodell auch nach Beendigung der Förderung durch den Sonderforschungsbereich weiter bis zur Fertigstellung seiner Dissertation im Februar 1977.

Finanzielle Förderung:

Jahr	Personal	Sächl. Verw. und Investitionen	Gesamtsumme
1970	1.231,74	19.557,56	20.789,30
1971	20.210,04	16.369,40	36.579,44
1972	54.775,62	12.251,01	67.026,63
1973	44.881,87	46.025,33	90.907,20
1974	57.178,93	15.928,47	73.107,40
1975	24.231,87	3.507,67	27.739,54
1976	-	-	
insgesamt	202.510,07	113.639,44	316.149,51

2. Dissertationen, Diplom- und Studienarbeiten

2.1 Westrich, B.: "Erosion eines gleichförmigen Sandbettes durch stationäre und pulsierende Strahlen", Dissertation, Universität Karlsruhe, Januar 1974.

2.2 Leister, P.: "Impuls- und Stofftransport in pulsierenden Drallstrahlen", Dissertation, Universität Karlsruhe, Januar 1977.

2.3 Schlenvoigt, G.: "Methoden der Schubspannungsmessung in rauhen Wänden", Diplomarbeit, Institut für Hydromechanik, Januar 1975.

3. Veröffentlichungen

Aus der Arbeit im Teilprojekt B 2 sind folgende Veröffentlichungen hervorgegangen:

3.1 Westrich, B. und Kobus, H.: "Erosion of a Uniform Sandbed by Continuous and Pulsating Jets", IAHR-Kongreß, Istanbul, August 1973.

3.2 Westrich, B.: "Influence of Seepage Flow and Velocity Pulsation in Jet-Erosion", Euromech 48, Kopenhagen, August 1974.

3.3 Kobus, H., Richter, A., Westrich, B.: "Aus der wasserbaulichen Forschung am Institut für Hydromechanik, Stauhaltung und Wasserversorgung", Zeitschrift für Binnenschiffahrt und Wasserstraßen, Heft 11, November 1975.

3.4 Westrich, B.: Discussion of: "Finite Element Model for Cohesive Sediment Transport", by R. Ariathurai und R.B. Krone, ASCE paper 11987, April 1976.

3.5 Leister, P.: "Experimental Investigation on the Turbulence Structure of an Impinging, Pulsating Jet", Proceedings, Symposium on Turbulent Shear Flows, Pennsylvania State University, USA, April 1977.

3.6 Kobus, H., Leister, P., Westrich, B.: "Flow Field and Scouring Effects of Continuous and Pulsating Jets Impinging on a Movable Bed", zur Veröffentlichung eingereicht an: Journal of Hydraulic Research, IAHR, 1977.

In Vorbereitung:

3.7 Leister, P.: "Influence of Surface Roughness on the Wall Shear Stress of Impinging Jets". Zur Einreichung bei: Wärme- und Stoffübertragung, Springer Verlag, Berlin.

3.8 Leister, P.: "Momentum and Mass Transfer in Impinging, Pulsating Jets". Zur Einreichung bei: Int. Journal of Heat & Masstransfer, Pergamon Press, Oxford, UK .

4. Vorträge

Folgende Vorträge wurden über die Arbeiten am Teilprojekt B 2 gehalten:

4.1 Kobus, H.: "Some Observations on Jet Erosion", Texas A. & M. University, College Station, Texas, USA, Juli 1974.

4.2 Westrich, B.: "Influence of Seepage Flow and Velocity Pulsation in Jet-Erosion", Euromech 48, Kopenhagen, August 1974.

4.3 Leister, P.: "Simultaneous Measurements of Wall Shear Stress and Relative Roughness of a Wall by a Double-Piped Preston-Tube", Euromech 61, Liverpool, April 1975.

4.4 Leister, P.: "Experimental Investigation on the Turbulence Structure of an Impinging, Pulsating Jet", Symposium on Turbulent Shear Flows, Pennsylvania State University, USA, April 1977.

4.5 Leister, P.: "Momentum and Mass Transfer in Impinging Pulsating Jets", Chemical Engineering Dept. University of Toronto, Kanada, April 1977.

5. Berichte

Folgende Fortschrittsberichte des Sonderforschungsbereichs sind zum Teilprojekt B 2 erschienen:

5.1 SFB 80/ET/17: Westrich, B., Kobus, H.: "Einfluß stationärer und pulsierender Strahlen auf die Erosion eines Sandbettes", März 1974.

5.2 SFB 80/T/54: Leister, P.: "Eichkurven für Preston-Rohre für Strömungen längs glatter und rauher Wände", Juli 1975.

5.3 SFB 80/ET/55: Leister, P.: "Einsatz einer Preston-Sonde mit Wandabstand zur Messung in rauhen Grenzschichten", Juli 1975.

5.4 SFB 80/ET/56: Leister, P.: "Simultane Bestimmung von relativer Rauhigkeit und Wandschubspannung in rauher Grenzschichtströmung mittels einer Doppelrohr-Prestonsonde", Juli 1976.

5.5 SFB 80/ET/66: Leister, P.: "Einfluß der Oberflächenrauhigkeit auf die Wandschubspannung von Prallstrahlen", Dezember 1975.

5.6 SFB 80/ET/85: Leister, P., Kobus, H.: "Impuls- und Stofftransport in pulsierenden Prallstrahlen", Dezember 1976.

5.7 SFB 80/ET/92: Kobus, H., Leister, P., Westrich, B.: "Flow Field and Scouring Effects of Steady and Pulsating Jets Impinging on a Movable Bed" (Abschlußbericht B 2), März 1977.

6. Schlußbemerkungen

Zur Abschätzung und Beurteilung der Erosionswirkung von Strahlströmungen, welche in der Praxis periodische Geschwindigkeitsschwankungen aufweisen können, ist es unerläßlich, sowohl die Erosionswirkung als auch die Strömungsverhältnisse genau zu kennen. Deshalb wurde im Rahmen des Teilprojekts B 2 die Erosionswirkung eines auf ein gleichförmiges Sandbett auftreffenden tiefgetauchten Strahls im Wassermodell quantifiziert, und zudem wurde in einem Luftmodell das Strömungsfeld eines auf eine ebene, rauhe Wand auftreffenden Prallstrahls ohne und mit Pulsation experimentell untersucht. Die Ergebnisse dienen der Klärung der Ursachen für die erhöhte Erosionswirkung pulsierender Strahlen und liefern gleichzeitig einen Beitrag zur Erforschung der Zusammenhänge zwischen periodischen und stochastischen Schwankungsbewegungen.

Die Erosionsuntersuchungen im Wassermodell wurden in den Jahren 1970 bis 1974 durchgeführt und sind in dem Bericht SFB 80/ET/17 ausführlich dar-

gestellt. Dieser Bericht enthält analytische Betrachtungen und umfangreiche experimentelle Untersuchungen der Erosionswirkung vertikaler Strahlen mit und ohne Pulsation. Die Experimente in einem Wassermodell mit gleichförmiger Sandsohle dienten der Ermittlung des zeitlichen Verlaufs der Kolkentwicklung.

In den ab 1973 in Angriff genommenen Untersuchungen am Luftmodell wurde das Geschwindigkeitsfeld des Prallstrahls sowie die Wanddruck- und Wandschubspannungsverteilung kontinuierlicher und pulsierender Strahlen sorgfältig untersucht. Insbesondere für die Messung der Wandschubspannungen an einer rauhen Wand mußte zunächst eine geeignete Meßmethode entwickelt und erprobt werden. Für die Bestimmung der Wandschubspannung mittels Prestonrohren wurden, unter Verwendung numerischer Berechnungsmethoden für das sogenannte Displacement, theoretische Eichkurven sowohl für glatte als auch für rauhe Grenzschichtströmungen hergeleitet, die im Bericht SFB 80/T/54 dargestellt sind. Eine speziell für Wandschubspannungsmessungen im Umlenk- und Wandstrahlbereich des Prallstrahls konstruierte Prestonsonde mit Wandabstand zur Messung in rauhen Grenzschichten wurde entwickelt und in einem geschlossenen Rechteckkanal geeicht; die Ergebnisse dieser Untersuchungen sind im Bericht SFB 80/ET/55 zusammengefaßt. Schließlich wurde eine Doppelrohrsonde mit zwei Rohren unterschiedlichen Durchmessers entwickelt, die die simultane Bestimmung von relativer Rauhigkeit und Wandschubspannung in einer rauhen Grenzschichtströmung ermöglicht. Die Grundlagen dieser Meßmethode und die Ergebnisse der durchgeführten Messungen zur Überprüfung sind im Bericht SFB 80/ET/56 dargestellt.

Mit Hilfe der neu entwickelten Meßmethoden wurde dann im Luftmodell der Einfluß der Oberflächenrauhigkeit auf die Wandschubspannung von Prallstrahlen experimentell ermittelt, wobei die Ergebnisse in dem Bericht SFB 80/ET/66 zusammengefaßt sind. Die umfangreichen Messungen am Luftmodell, in denen nicht nur die zeitlich gemittelten hydrodynamischen Größen und die momentanen Schwankungsbewegungen sondern auch - im Hinblick auf eine mögliche Anwendung in der Verfahrenstechnik - der Stoffübergang erfaßt wurde, sind in dem Bericht SFB 80/ET/85 ausführlich dargestellt und im Detail diskutiert.

Schließlich enthält der hier vorliegende Bericht SFB 80/ET/92 eine Zusammenfassung der wesentlichen Ergebnisse des Forschungsprojekts, wobei die Erosionswirkung kontinuierlicher und pulsierender Prallstrahlen aus der Kenntnis des Strömungsfeldes insgesamt erklärbar wird. Damit liegen quantitative Angaben über die Erosionskapazität stationärer und pulsierender Prallstrahlen vor. Durch die Kenntnis des Strömungsfeldes aus dem Luftmodell wird ein direkter Bezug zum Erosionsvorgang, der im Wassermodell untersucht wurde, hergestellt. Hierbei wird plausibel gezeigt, daß durch die erhöhte Korrelation der Schwankungsbewegungen infolge Pulsation der Erosions- und Transportvorgang beschleunigt wird.

Dieser zusammenfassende Abschlußbericht ist in englischer Sprache abgefaßt, da er gleichzeitig zur Veröffentlichung an das Journal of Hydraulic Research der International Association of Hydraulic Research eingereicht wird. Dadurch soll erreicht werden, daß die internationale Fachwelt über die wesentlichen Ergebnisse dieses Forschungsvorhabens unterrichtet wird.

TEIL B

FLOW FIELD AND SCOURING EFFECTS OF STEADY AND PULSATING JETS IMPINGING ON A MOVABLE BED

Dieser Teil des Abschlußberichts ist
zur Veröffentlichung eingereicht an

"Journal of Hydraulic Research"

(International Association for Hydraulic Research)

List of Symbols

A	Constant
d_o	nozzle diameter
d_s	mean grain diameter
f	pulsation frequency
k_o	pressure parameter
k_f	Darcy permeability
k_s	equivalent sandroughness
ℓ_o	nozzle to wall distance
M_o	momentum flux
n	exponent of Re-number
P_w	wall pressure
p_s	stagnation pressure, $p_s = \bar{p}_w \quad (r = o)$
r_o	nominal scour radius
Re_o	nozzle Reynolds number $\equiv \frac{u_o \cdot d_o}{\nu}$
Re_s	grain Reynolds number $\equiv \frac{w \cdot d_s}{\nu}$
r	radial coordinate
Sr	Strouhal number $\equiv \frac{f \cdot d_o}{\bar{u}_o}$
t	scouring time
u	velocity in x-direction
u_f	seepage velocity
z	separation from wall
z_o	maximum depth of scour
α	amplitude of pulsation
δ	thickness of boundary layer
φ	azimuthal angle
ν	kinematic viscosity
ρ	density
τ	wall shear stress

subscripts:

a	center line	s	sand
f	Darcy	$\propto$	proportional
o	nozzle	$\approx$	about the same value

1. INTRODUCTION

Jets impinging on a movable bed of particles can lead to strong local scouring effects. Submerged jets, which in practice frequently show periodical velocity fluctuations, can either lead to dangerous scouring near hydraulic structures, or be put to technical use due to their strong erosion capacity. Unwanted effects are found, for example, in the erosion of the bottom of navigable waterways by ship propellers, whereas in dredging high velocity jets are successfully used for loosening hardpacked sandy soils, or also for submarine underground-laying of pipes. Furthermore, the flow field of impinging jets is of interest for hovercrafts and for vertical takeoffs, and also for numerous applications in chemical engineering.

In order to control the wanted or unwanted scouring effects of impinging jets, it is necessary to know in detail both the flow field and the scouring effect of this flow configuration. Therefore, an experimental investigation of an axi-symmetrical, vertical, submerged jet impinging on a horizontal sand bed of uniform grain size was studied. Particular attention was paid to the quantification of the influence of a pulsation of the jet velocity, which under certain geometrical and flow conditions causes an increase of the scouring rates.

The flow configuration investigated, as it exists at the beginning of the erosion process, is sketched in Figure 1. For reasons of experimental techniques, this configuration was studied both in an air- and in a water model: whereas the flow field can be measured more easily in air by means of hot-wire techniques, it is more realistic to investigate the erosion process in water, where the same density ratio can be achieved as in the prototype. Therefore, the following complementary experiments were conducted:

- in the air model, the flow field of a vertical turbulent jet impinging on a horizontal rough and unerodible wall was investigated. This configuration corresponds to the initial phase of the erosion process (scouring time $t = 0$). Preference was given to the flat plate configuration instead of a fully developed scouring hole, because the former corresponds to a simpler case, for which literature data for smooth walls are available for comparison.

- In the corresponding water model, the erosion process of a sand bed of uniform grain size due to a turbulent submerged jet was quantitatively evaluated for the same geometrical initial conditions (horizontal bed) and for various grain sizes of the sand.

The flow field and the (time-dependent) erosion process is characterized by the jet parameters (momentum flux M_o and distance ℓ_o from the bed) on the one hand and the parameters of the bed material (representative grain diameter d_s or equivalent sand roughness k_s and fall velocity w) on the other. In pulsating jets, the amplitude α and the frequency f of the pulsation must be considered in addition. A dimensional analysis yields the following general relationship (definitions see Figure 1):

$$\begin{matrix}\text{Flow field} \\ \text{Erosion process}\end{matrix} = f_{1/2}\left[Re_o = \frac{\bar{u}_o d_o}{\nu}; \frac{\ell_o}{d_o}; \underset{Re_s}{k_s/d_o}; \frac{\bar{u}_o}{w}; Sr = \frac{f\, d_o}{\bar{u}_o}; \alpha\right] \qquad (1)$$

This relationship is limited to vertical, axially symmetrical turbulent jets and non-cohesive bed materials of uniform grain size.

For the investigations of the flow field in the fixed-bed air model the roughness is described by the equivalent sand roughness k_s according to Nikuradse, whereas the fall velocity w is of no significance. For investigations of the flow field of impinging jets, one obtains therefore:

$$\text{Flow field} = f\left[Re_o; \frac{\ell_o}{d_o}; \frac{k_s}{d_o}; Sr; \alpha\right] \qquad (2)$$

Experimental range:

Re_o	: from $2 \cdot 10^4$ to $6 \cdot 10^4$	(mainly $6 \cdot 10^4$)
ℓ_o/d_o	: from 11.6 to 16.6	(mainly 16.6)
k_s/d_o	: from 0 to 0.0833	
Sr	: from 0 to $6 \cdot 10^{-2}$	
α	: from 0 to 0.70	

For the erosion experiments with movable bed fully turbulent flow can always be assumed and therefore the Reynolds number of the jet has no significance (The Reynolds numbers in the water investigations ranged from 3 to 18 x 10^4).

In this case, one obtains

$$\text{Erosion process} = f\left[\frac{\ell_o}{d_o}; Re_s; \frac{\bar{u}_o}{w}; Sr; \alpha\right] \qquad (3)$$

Experimental range:

ℓ_o/d_o : from 1.6 to 41 (mainly 14.5)
Re_s : from 140 to 900
$\bar{u}_o/w$: from 6.1 to 30
Sr : from 0.022 to 0.272
α : from 0 to 0.81 (mainly 0.5)

2. FLOW FIELD OF IMPINGING STEADY JETS

Impinging jets exhibit four different flow regions (Figure 1). Immediately downstream of the nozzle, a potential core exists, which rapidly diminishes in the downstream direction due to the shear stresses between the receiving fluid and the jet. After a more or less well-defined transition zone, a free-jet region follows, which is characterized by similarity of the velocity profiles. Near the wall, an impinging region forms, where the flow is translated from axial into radial motion, which is connected with the formation of a pressure field. The deflected flow continues as a wall jet, which contains two different shear zones: a boundary layer near the wall, in which the velocity increases from zero at the wall to the maximum value of the wall jet, and a free-shear zone, in which the jet velocity decreases again. Wall jets also show similarity profiles for the velocity distribution.

The main parameters characterizing the flow along the wall are the wall pressure, the wall shear stress and the maximum velocity parallel to the wall. For smooth walls, both theoretical and experimental information is available in the literature for these parameters. The most important results are summarized in the papers of Glauert (1), Bradshaw and Love (2), and Poreh and Cermak (3) as well as in a more recent summary by Rajaratnam (4). No systematic investigations are available of the influence of the wall roughness on the flow field. Sandborn and Chao (5) report about velocity measurements in the wall-jet region

near an artificially roughened wall, whereas Lam Lau (6) and Jayatillike (7) conducted such measurements on walls with sandpaper roughness. About the profiles for wall pressure and wall shear stress at a rough wall, no data are available so far.

Leister (8) investigated the influence of wall roughness on the distribution of wall pressure, wall shear stress and the velocity field in the wall-jet region for the parameters defined in Chapter 1. The measurements of wall pressure and wall shear stress were taken by means of a modified Preston probe, whereas for velocity measurements both a direction-sensitive Pitot probe and a constant-temperature hot-wire anemometer were used. The experimental arrangement and measurement techniques are described in detail in (8).

The measurements showed that the distribution of wall pressures is not influenced by the roughness as long as the roughness height is small in comparison to the dimensions of the deflection region. It can be shown (8) that the dimensionless wall-pressure distribution can be described with the aid of a single experimental constant to:

$$\frac{\bar{p}_w(r/\ell_o)}{\rho\frac{\bar{u}_\delta^2}{2}(\ell_o/d_o)^2} = A\exp\left[-2A(r/\ell_o)^2\right] \qquad ; A=57.0 \qquad (4)$$

The wall shear distribution, on the other hand, is influenced strongly by the roughness. Both in the deflection region, which shows a linear increase of the wall shear stress with radial distance, and in the wall-jet region, where the wall shear stress decays exponentially, the wall shear stress is increased with increasing wall roughness; the location of the maximum wall shear stress is shifted slightly towards the stagnation point. In Figure 2, which shows the dimensionless wall shear distribution, the influence of the roughness parameter is clearly visible in the staggering of the experimental points. The similarity of these experimental curves indicates that the similarity behavior of the flow field is only modified by the wall roughness as compared to the field above a smooth wall. The shear stress distributions for smooth and rough walls can be described by the following empirical relationships (with an established validity range as given by the experiments):

$$\frac{\bar{\tau}_{o\,rough}}{\bar{\tau}_{o\,smooth}} = \left[7.43\left(\frac{k_s}{d_o}\right)^{.412} \exp\left[-7.8\left(r/\ell_o\right)+1\right]\right] Re^{.045}$$

with (5)

$$\frac{\bar{\tau}_{o\,smooth}}{\rho\frac{\bar{u}_o^2}{2}(\ell_o/d_o)^2} = \frac{.082}{r/\ell_o} - \exp\left[-22.7(r/\ell_o)^2\right] \left(\frac{.082-13.4(r/\ell_o)^2}{r/\ell_o}\right) Re_o^{-.165}$$

The effect of the wall roughness on the flow field is shown in Figure 3. A comparison of the profiles for smooth and for rough walls indicates clearly that the velocities are decaying more rapidly with distance from the stagnation point near the rough wall as compared to the smooth wall, which is connected with a more rapid increase of the boundary-layer thickness, characterized by the shifting of the points of maximum velocity away from the wall.

The behavior of the axial stochastic turbulence components is changed in the boundary layer by the wall roughness insofar as the intensities in the immediate vicinity of the wall are increased as compared to a smooth wall. However, the roughness has no influence on the turbulence characteristics in the free-shear zone (see Figure 3).

3. SCOURING DUE TO IMPINGING STEADY JETS

Investigations on the erosion capacity of steady jets have been conducted by Poreh, Hefez (12), Rouse (13) and Altinbilek and Okyay (14) with vertical jets, whereas Laursen (15) and O'Loughlin and others (16) have studied the erosion capacity of weakly inclined jets and jets parallel to the bed. The laboratory investigations served primarily the purpose to establish the time dependence for local erosion problems and to aid in developing similarity criteria for scouring problems in hydraulic models. The importance of the pressure- and velocity field near the bed or the importance of the permeability of the bed for the erosion process has not yet been explored.

The time development of bed deformation can be well described by a logarithmic law. A semi-logarithmic presentation of the erosion process shows two distinct phases, during each of which the eroded scouring volume is proportional to the logarithm of erosion time (Figure 4). This time dependence shows that the erosion rate, defined by the growth rate of the scour volume, is proportional to the

logarithm of the erosion time in both scouring phases I and II. The maximum erosion rate is reached immediately after initiating the erosion process ($t \geq 0$), when the bed is still horizontal and most of the jet energy can be translated into erosion and transport work. Since the erosion power of a jet can be quantified in terms of the erosion rate, this quantity can serve as a basis for comparing steady and pulsating jets.

For the analysis of the erosion of a sandbed by jets, the wall must be replaced by a pervious porous medium. For an impervious bed, the stagnation pressure p_s is proportional to the square of the fictitious centerline velocity $u_{m,\ell}$ of the submerged free jet at a distance ℓ_o from the nozzle, which in turn is proportional to the nozzle-exit velocity u_o:

$$p_s = p_w(r=0) \propto \frac{\rho}{2} u_{m,\ell}^2 \propto \frac{\rho}{2} u_o^2 \tag{6}$$

For a pervious erodible bed, the magnitude of the stagnation pressure is furthermore dependent on the shape of the bed profile and the Reynolds number of the grain, which characterizes the degree of infiltration. Figure 5 qualitatively shows the influence of the permeability of the bed material on the pressure- and velocity profile in the deflection- and wall-jet region, as compared to the situation for an impervious bed. With increasing permeability, the actual stagnation pressure is reduced and the radial velocities as well as the resulting bed shear stresses are also diminished, since not the entire longitudiual jet momentum is converted into radial momentum. The more energy is put into the seepage motion, the smaller is the remaining energy for erosion and transport of the bed material, since the seepage flow does not contribute to the hydromechanical erosion (17). The influence of the seepage velocity increases with increasing permeability k_f (according to Darcy) and with increasing gradient of the piezometric head in the plain of the bed:

$$u_{fo} = k_f \frac{\partial h}{\partial s} \sim k_f \frac{p_s/g\rho}{b} \tag{7}$$

where b is the (fictitious) nominal width of the free jet in the plane of the undisturbed bed. With increasing ratio of seepage velocity to stagnation

$$\frac{u_{fo}}{\sqrt{p_s/\rho}} \sim \frac{k_f}{bg}\sqrt{p_s/\rho} \tag{8}$$

pressure head, more and more energy is being dissipated in the sediment bed without any effect on the erosion. This finally leads to the jet injection configuration, in which almost the entire jet energy is dissipated in the seepage flow.

For a given grain size, the erosion process is uniquely dependent upon the geometrical and flow parameters at the beginning of erosion (t = 0, horizontal bed). Therefore, the erosion process can be described as a function of the pressure distribution of the impinging jet at a horizontal bed. Since the real pressure distribution at the beginning of the erosion is defined by the pressure field for an impervious rough bed and by the permeability of the bed, which depends on the grain size, the erosion problem can be uniquely correlated with the pressure field given by equation (4) and the properties of the grains. Therefore, the erosion process can be described as a function of the pressure parameter k_o,

$$k_o = \frac{p_s}{\frac{\rho}{2} w^2} \propto \frac{u_m^2}{w^2} \qquad (9)$$

and of the Reynolds number of the grain ($Re_s = w\, d_s / \nu = 140$).

If the pressure parameter k_o at the beginning of erosion does not exceed a certain limiting value, which depends upon the sediment bed ($k_o \leq 0.025$), then for the entire erosion process, the scouring form I will form, which is shown in Figure 6. The universal similarity profile I is characterized by the fact that the deflected jet is attached to the bed along the entire erosion zone. Only at the edge of the scour hole, at a distance ($r = r_o$), separation occurs due to the bed deformation, which, however has no influence on the erosion. The bed material is put in motion in the entire deflection zone and is transported radially outward as bedload. The scour radius r_o as the maximum transport distance is independent of time and governed exclusively by the width of the pressure field, which according to eq. (4) is proportional to the nozzle distance ℓ_o for ($\ell_o > d$). The maximum scouring depth z_o, on the other hand, increases both with the pressure parameter and with the erosion time, and finally approaches an asymptotic limiting value. Scouring form II (see Fig. 6) is characterized by a pronounced bed deformation in the center of the jet (inner region) and by an outer region with a straight slope up to the edge of the scour hole, which is determined by the inner angle of friction of the bed material. Due to the shape of the bed profile, flow separation occurs at the edge of the inner region. Under the given flow conditions,

the bed material is eroded exclusively in the inner region, whereas beyond the separation point it is transported in suspension by the separated wall jet radially outward, and finally deposited. The similarity profile II is a time-independent, dynamically stable configuration, which is a function of the pressure parameter k_o. With increasing values of k_o, the depth in the center of the scour hole is increased. For extreme values of the pressure coefficient, the erosion is finally replaced by an injection flow, in which the scour shape II is deformed into an extremely deep hole in the jet center.

A jet with a given exit velocity v_o and nozzle diameter d_o shows an erosion capacity which is strongly dependent on the nozzle distance ℓ_o from the bed, as can be seen from the relationship between the relative scour volume and the distance parameter in Figure 7. The maximum erosion capacity is always obtained at large nozzle distances, where the pressure parameter reaches a value of about 2.2, and no separation of the deflected jet is found. With decreasing nozzle distance, stronger pressure gradients in the deflection region yield a stronger jet deflection, and a larger portion of the energy is dissipated into the seepage flow, so that the erosion capacity is decreasing rapidly after showing a second relative maximum at $k_o \approx 8.4$.

A change in the jet velocity causes a change in the stagnation pressure, but no change in the width of the pressure field at the bed. An increase of the jet velocity, therefore, increases the erosion potential of the jet, which reflects in both scouring phases, in an increase of the erosion rate (Figure 7). In the intermediate velocity range (v_o/w from 14 to 24), one finds a pronounced deformation of the bed, which causes an increased energy dissipation and a decrease of the erosion and transport efficiency of the jet, so that the erosion capacity remains practically constant inspite of the increased jet power. Only a further increase of the jet velocity ($v_o/w > 25$) can yield a further increase of the erosion rate.

The experimental investigations of the flow field and the erosion capacity of an impinging jet have shown that there is a strong feedback between flow and erosion. The erosion process including positive and negative feedback mechanisms

can be shown in the form of a block diagram (Figure 8). One can talk about jet erosion only for pressure values k_o in the range of about 1.2 up to about 140. The larger the value of the pressure parameter, the earlier one reaches a deflection angle of more than 90° and, thus, the scour form II. With increasing pressure parameter, the deflection angle of the jet increases up to values of 180°. The angle of the deflected flow thus becomes more and more unfavorable, and a large portion of the eroded material is entrained directly again into the downward jet and thus does not contribute to the scouring rate. Only a minor part of the eroded material reaches the radial transport flow and is transported towards the edge of the scour hole. The material deposited on the inner flanks of the scour hole is sliding gradually towards the erosion center and is there picked up again by the flow (positive feedback). All grains, which have passed a control section at the distance $r = r_o$ contribute to the erosion process and thus are eliminated from the internal flow; they cause a deepening of the center of the scour hole and thus a decrease of the shear stresses at the bed (negative feedback). When the scour hole has reached similarity conditions, then there exists a dynamic balance between flow and bed form, in which the transport capacity of the radially deflected flow shows a constant ratio to the erosion capacity in the center. The scour hole increases with time while maintaining a constant scour shape and flow configuration, until finally, after extremely long erosion times, an asymptotic value is reached in deviation from the logarithmic time law. This asymptotic value, however, could not be verified experimentally because of the required extreme duration of such an experiment.

4. PULSATION EFFECTS ON THE FLOW FIELD

Velocity pulsations which are superimposed on the mean exit velocity at the nozzle have an influence on the flow field in all regions. Investigations of pulsating free jets by Favre-Marinet (9), Remke (10) and Olivari (11) show that pulsating jets exhibit a larger spreading angle and at the same time a more rapid decrease of the axial velocity, and that they attain similarity of the mean velocity profiles, after comparatively small nozzle distances. However, the available data do not allow to establish a quantitative relationship between the observed effects and the pulsation parameters.

For the experimental investigation of the behavior of impinging jets and of the influence of the pulsation, the pulsation parameters have been varied in the range of amplitude parameters α from 0 to 70 per cent, and Strouhal numbers Sr up to $6 \cdot 10^{-2}$. Comparisons between steady and pulsating jets were made on the basis of equal mean momentum flux at the nozzle. The results of these investigations can be summarized as follows: Above a certain lower limit of the Strouhal number, the wall pressure at the stagnation point is decreasing, whereas the pressure field becomes comparatively wider, so that in the order of the deflection region the wall pressure can be higher in the pulsating jet than in the steady jet. This effect is becoming more pronounced with increasing frequency (Fig. 9). The effect of the pulsation amplitude is of secondary importance for the pressure field. The pressure distribution for a pulsating jet can be described in dimensionless form by a comparatively simple relationship:

$$\frac{\bar{p}_{w\ pulsating}}{p_{w\ steady}} = 1 - 60.3\ Sr^{1.53} \exp\left[-1.68 \times 10^{-3} (r/\ell_o)^2\ Sr\right] \qquad (10)$$

Correspondingly, the mean wall shear stresses exhibit a similar trend for Strouhal numbers above a certain lower limit, with the wall shear stress in the deflection region and in the initial part of the wall jet region decreasing with increasing Strouhal number. The point of maximum shear stress is shifted slightly away from the stagnation point. In the wall-jet region, the decrease of the wall shear stress is less gradual for the pulsating jet, so that at large distances from the stagnation point, the values of the shear stress show no distinction for steady and pulsating jets (Figure 9). Here also, the pulsation amplitude is of secondary importance. The dependence of the shear stress distribution in the deflection region and in the initial part of the wall-jet region upon the pulsation parameters can be described by the following equation:

$$\frac{\bar{\tau}_{o\ pulsating}}{\bar{\tau}_{o\ steady}} = \left(1 - 3.75\ Sr^{0.42} \alpha^{0.15} \exp\left[-7.46\ r/\ell_o\right]\right) 0{,}078\ Re_o^{n_p} \qquad (11)$$

where the exponent n_p seams to depend upon the Reynolds number (8).

The results for the wall shear stress are in accordance with measurements of the maximum velocity parallel to the wall, which is decreasing more slowly in the wall-jet region of the pulsating jet as compared to the steady jet (Figure 11).

The velocity profiles in the wall-jet region show similarity behavior even under pulsation.

For a description of the turbulence structure of the flow field of the pulsation jet, hot-wire measurements have been performed and analyzed by means of auto- and cross-correlation. By correlation techniques, periodic parts can be separated from the stochastic parts of the signal, and thus the mutual interrelationship of periodic and stochastic components can be quantified. Measurements have been taken both in the boundary layer near the wall and in the free-shear zone of the wall jet. Figure 12 shows two-point correlations of the radial fluctuations at the beginning of the wall-jet region, that is at the point of maximum wall shear stress. For these measurements, one probe was mounted at $z = 2\,k_s$, whereas the second probe was traversed at the same elevation around the circumference. For a steady impinging jet, this two-point correlation

$$R_\varphi^* = \frac{\overline{v(r=r_m;\, z=2k_s;\, \varphi=0;\, t)\cdot v(r=r_m;\, z=2k_s;\, \varphi>0;\, t)}}{\overline{v^2(r=r_m;\, z=2k_s;\, \varphi=0;\, t)}} \qquad (12)$$

decreases rapidly (Fig. 12) with increasing separation angle of the probes, which means that the instantaneous fluctuating components in the radial outward direction, which are mainly responsible for the erosion and the transport of bed material, are not particularly well correlated. In contrast, the pulsating jet shows a strong correlation of these radial fluctuating components over the entire circumference, which means that there exist well-correlated fluctuating components in the outward direction around the entire circumference.

The separation of the fluctuating components into periodic and stochastic parts showed for the radial fluctuations in the boundary layer near the wall, that there is no interference of these components, which means that the turbulence structure within the wall boundary layer is not changed by the pulsation (Fig. 13). In the free-shear layer of the wall jet, on the other hand, the velocity pulsations interfere primarily with those turbulence elements (eddies) which have a frequency corresponding to the pulsation frequency. By this process, the periodic motion feeds energy into these large eddies and thus prolongs their duration of existence. Intensity measurements of the total fluctuations in the free-shear

zone show that the pulsating jet exhibits an increased total fluctuation (Fig. 14). The respective contribution of periodic and stochastic parts to the total fluctuation has been determined and is given in (8).

5. PULSATION EFFECTS ON THE SCOURING PROCESS

Knowledge of influence of velocity pulsations upon the flow field of an impinging jet on an impermeable wall allows some conclusions concerning the influence of the pulsation upon the erosion process. Since the pulsation leads to a decrease of the velocity on the jet axis, and thus to a wider pressure field, the deflection region is increased in width. At the same time, the induced seepage velocity in the sediment bed for permeable bed material is diminished because the pressure gradient is smaller, so that an increased erosion action can be expected because of the decreased holding forces of the grain.

The pulsation does not only influence the erosion because of the changes of the mean flow field, but also by the changes of the turbulence characteristics. The strong correlation of the fluctuating components is of particular importance both for the instantaneously increased attack on the grain bed and for a more efficient transport of the particles in suspension from the erosion zone to the outer edge of the scour hole. By a simplified consideration for a single grain it can be demonstrated how the erosion and the transport of the bed material is influenced by the turbulence characteristics as changed by the pulsation. In order to set a grain in motion by fluid dynamic forces in the turbulent boundary layer, the driving dynamic force must be larger than the retaining friction force and the retarding inertial force of the grain including the surrounding fluid (added mass) and the component of the gravitational force of the submerged grain. In order to retain the grain in motion and not let it slide back into its initial position, but transport it at least by rolling over the neighboring grain, the fluid dynamic force must be acting for a certain minimum duration time, which depends upon the turbulent fluctuations. Since the resulting direction of transport is given by the mean radial flow, the flow shows a greater efficiency when the direction of the resulting fluid dynamic force coincides with the radial direction. The stronger

the correlation of the force fluctuations in the direction of the transport is along a circular circumference, the more turbulent energy can be transformed into erosion- and transport capacity. Since the driving fluid dynamic force corresponds to the integral over the pressure on the grain surface, and since this pressure is influenced by the turbulent fluctuations, the correlation of the radial velocity fluctuations over the circumference gives an indication of the orderly attack of the fluctuating flow components. As the pulsating jet has considerably higher correlation in the radial direction than the steady jet of equal mean momentum- or mass flux at the nozzle (Figure 12), the forces on the grains due to turbulence are directed more strongly in the radial direction and are less random due to the pulsation. The stronger correlation thus has the consequence that the flow is more effective with regard to erosion and transport of the grains.. For certain grain sizes, the efficiency of the pulsation can furthermore be increased by choosing frequencies of the pulsation which are in the range where the specific work necessary for setting a grain into motion is smaller than for a statistically random turbulence spectral distribution of the same total energy content.

Since pulsations at the nozzle change the distribution of mean pressure and velocity profiles at the bed considerably in comparison to the steady jet, the erosion process takes place under different initial and boundary conditions. The changes of the mean velocity profiles in the free jet region are comparable qualitatively, concerning their effect on the erosion, with a steady jet of equal momentum flux, but increased nozzle distance from the bed. The effect of the pulsation on the increase of the erosion rate is a maximum when the change in flow conditions leads to a shift from scour form II to form I. It becomes evident from Figure 4, that the erosion process is different from the case of the steady jet insofar as the erosion rate is increased both in phase I and phase II of the scouring process. Since phase II is the phase of main importance for practical applications, and since it can be described sufficiently accurately, this phase will serve as a basis of comparison for the erosion capacity of both types of jets.

Figure 15 shows the ratio of the erosion rates for pulsating and steady jets in scouring phase II for various frequency and amplitude parameters. The erosion rate of a pulsating jet is increasing with increasing frequency and amplitude of

the pulsation. The degree of increase of erosion is strongly dependent upon the velocity and distance parameters ($\bar{u}_o/w$, ℓ/d_o) , as can be seen clearly in the three-dimensional plot given in Figure 16. The absolute maximum increase of the erosion rate due to pulsation, which has been observed for quartz sand with k_o = 140, occurred at a distance parameter ℓ/d_o of around 12 and a velocity parameter $\bar{u}_o/w$ of about 16. Under these conditions, the pressure parameter k_o is influenced in an optimal fashion, so that the erosion process is increased substantially in comparison to a steady jet of the same mean momentum flux.

6. CONCLUSIONS

The mean and fluctuating components of the flow field of vertical submerged jets impinging on a horizontal rough wall have been measured, and the time-development of scour holes due to submerged jets impinging on sand beds of uniform grain size has been studied experimentally. Particular attention has been paid to the quantification of pulsation effects upon the flow field and the scouring process. The results allow quantitative assessment of the various parameters upon the scouring process for steady and pulsating jets. In particular, the following general conclusions can be derived from the study:

- The scouring process has a logarithmic time dependence,
- The erosion capacity of a jet depends upon its momentum flux, the nozzle distance from the bed, and the properties of the bed material,
- Depending on the magnitude of the pressure parameter $k_o = p_s / \frac{\rho}{2} W^2$, different scour forms may be generated. For small values of $k_o (1.2 \lesssim k_o \leq 3)$ one obtains form I, for larger values of k_o $(6.5 \lesssim k_o < 140)$ the form II, whereas very large values of k_o lead to injection flow,
- Scour form I shows a shallow profile, in which the wall jet is attached up to the edge of the scour hole. Erosion takes place mainly in the form of bedload transport.
- Scour form II exhibits a strong deformation in the inner region, where erosion takes place, and straight flanks in the outer region of the scour hole, in which transport in suspension and partial deposition take place.

- Periodic pulsation of the jet can cause a significant increase of the erosion capacity. This is due to the following factors:

  + more favorable erosion- and transport conditions in the deflected jet due to a diminished pressure gradient along the bed;

  + decreased energy loss of the mean radial transport flow due to the less intensive separation of the deflected jet;

  + smaller energy loss into the seepage flow on account of the reduction of the pressure gradient, which reduces the seepage flow;

  + better efficiency of the turbulent transport because of the pronounced radial correlation of the radial velocity components around the circumference.

REFERENCES

1 Glauert, M.B.: "The wall jet", Journal of Fluid Mechanics 1 (1956) pp 625/643

2 Bradshaw, P. and Love, E.M.: "The normal impingement of a circular air jet on a flat surface", Aeronoutical research council reports and memorandum No.3205, 1959.

3 Poreh, M. et al.: "Investigation of a turbulent radial wall jet", Journal of Applied Mechanics (1967) pp 457/463.

4 Rajaratnam, N.: "Turbulent Jets", Elsevier Scientific Publishing, Amsterdam - New York - Oxford, 1976.

5 Sandborn, V.A. and Chao, J.L.: "Evaluation of the momentum equation for a turbulent wall jet", Journal of Fluid Mechanics, Vol.26 (1966) 4 pp 819/828.

6 Lam Lau: "Flow characteristics of wall-jets on smooth rough and porous walls", Department of Mechanical Engineering University of Toronto, Canada, Master Thesis, 1963.

7 Jayatilleke, C.L.V.: "The influence of Prandtl number and surface roughness on the resistance of the laminar sub-layer to momentum and heat transfer", Progress in Heat and Mass Transfer 1 (1969) pp 193/329.

8 Leister, P.: "Momentum and mass transfer in impinging, pulsating jets", University of Karlsruhe, Dissertation, February 1977 (in German).

9 Favre-Marinet, M. et al.: "Jets instationaires", Etude No.2, Structure Des Jets Pulsants, Universitée Grenoble, Octobre 1971 et Juin 1972.

10 Remke, K.: "Untersuchungen an pulsierenden turbulenten Freistrahlen", Mitteilungen des Instituts für angewandte Mathematik und Mechanik, Universität Berlin (DDR) 1972

11 Olivari, D.: "Analysis of an axisymmetrical turbulent pulsating jet", Von Kharuan Institute for Fluid Dynamics, Technical Note 104 (1974).

12 Poreh, M. and Hefez, E.: "Initial scour and sediment motion due to an impinging submerged jet", IAHR, Fort Collins, USA, Vol.3 1967.

13 Rouse, H.: "Criteria for Similarity in the Transportation of Sediment", Proc. of Hydr. Conf., Pasadena, 1942.

14 Altinbilek, H., Okyay, S.: "Localized Scour in a Horizontal Sand Bed under Vertical Jets", IAHR, Instanbul, 1973

15 Laursen, E.: "Observation on the Nature of Scour", Proc. 5th Hydr. Conf. publ. by the University of Iowa, No.426, June 1952.

16 O Loughlin, E.M. et al.: "Scale Effects in Hydraulic Model Tests of Rock Protected Structures", IAHR Rep., Iowa Inst. of Hydr.Res., February 1970.

17 Westrich, B.: "Influence of Seepage Flow and Velocity Pulsations in Jet-Erosion", EUROMECH 48, Kopenhagen, 1974.

LIST OF FIGURES

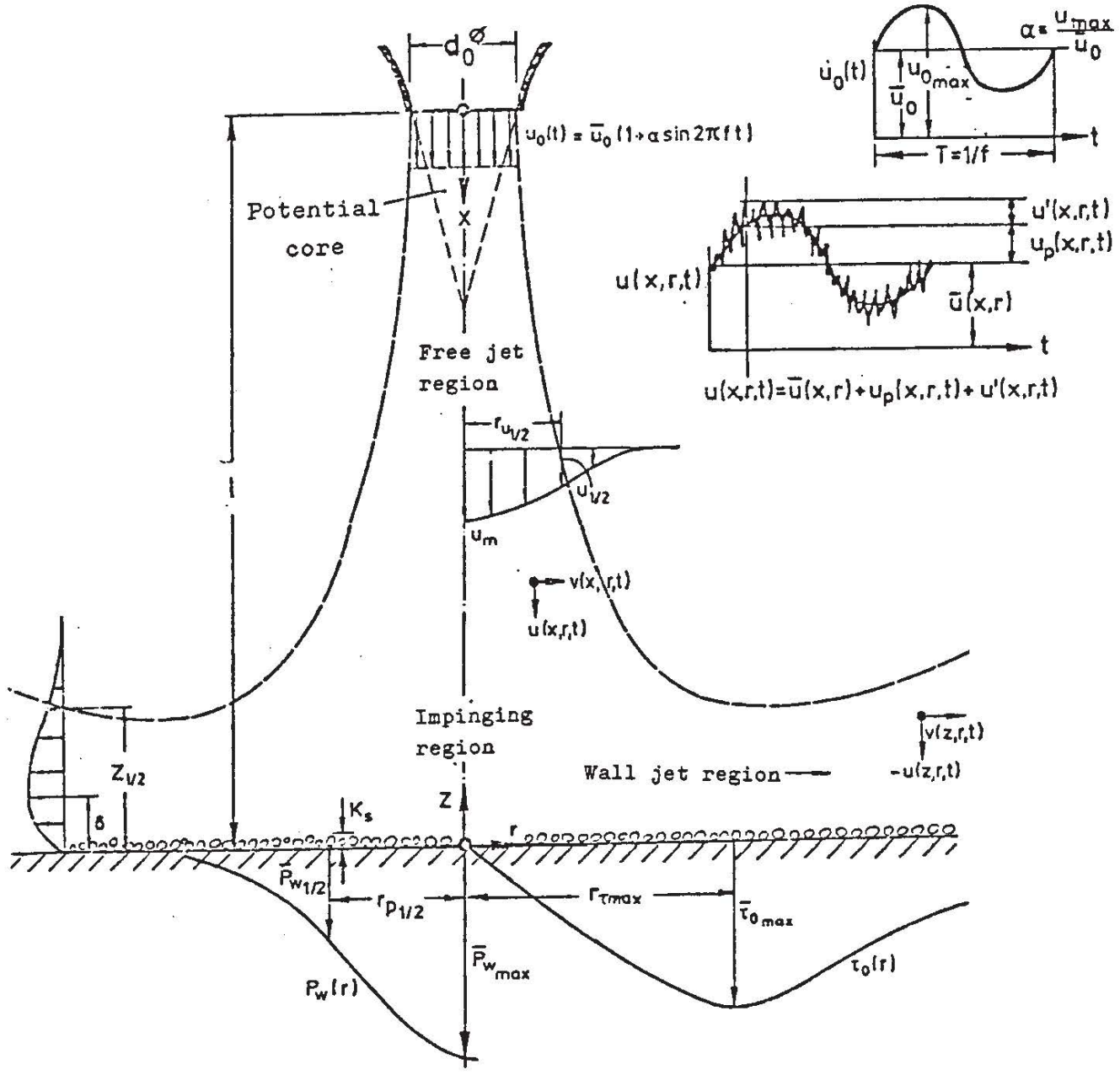

SFB 80 B 2	Definition sketch of an impinging jet	1

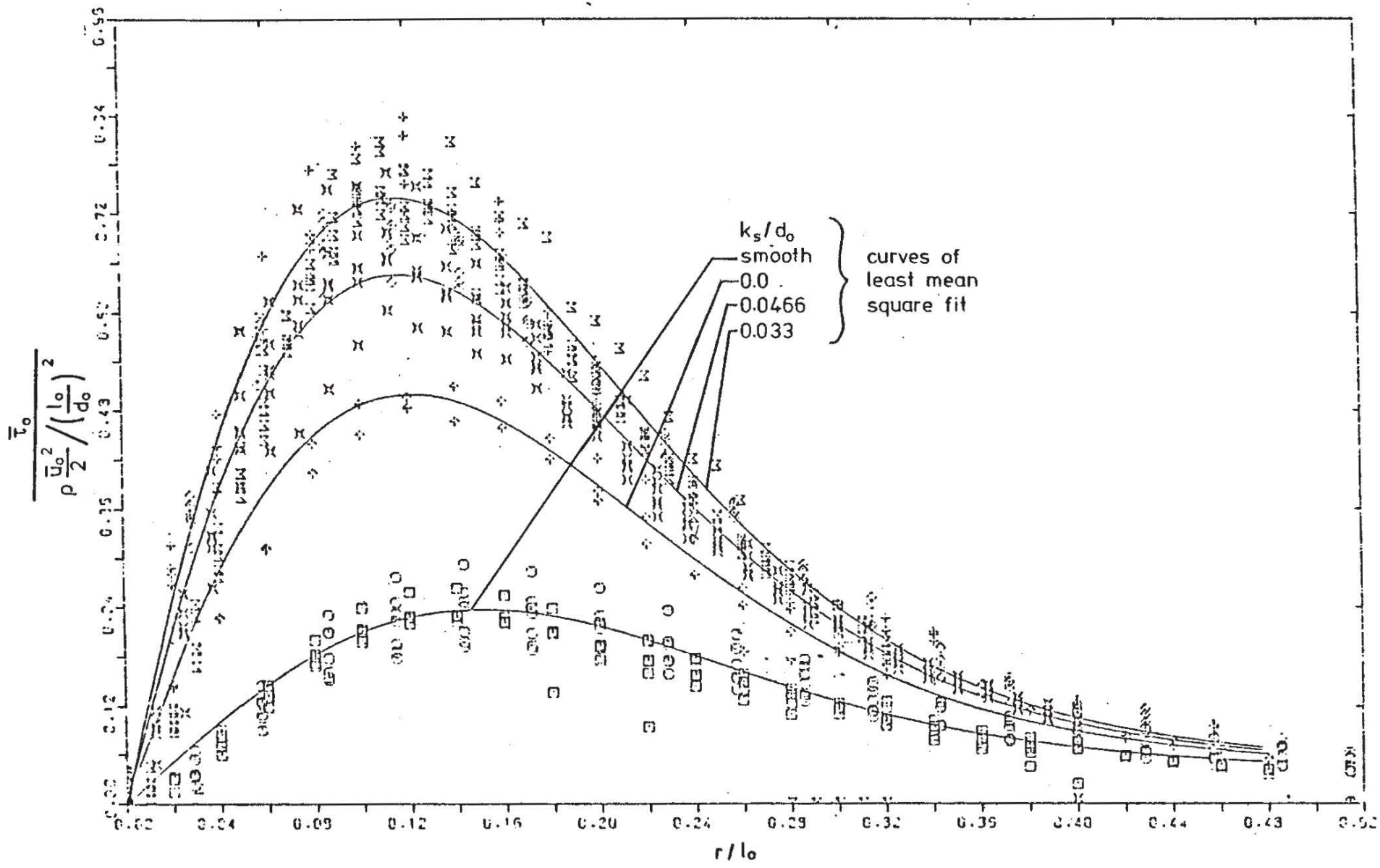

SFB 80 B 2	Influence of wall roughness on the wall shear stress	2

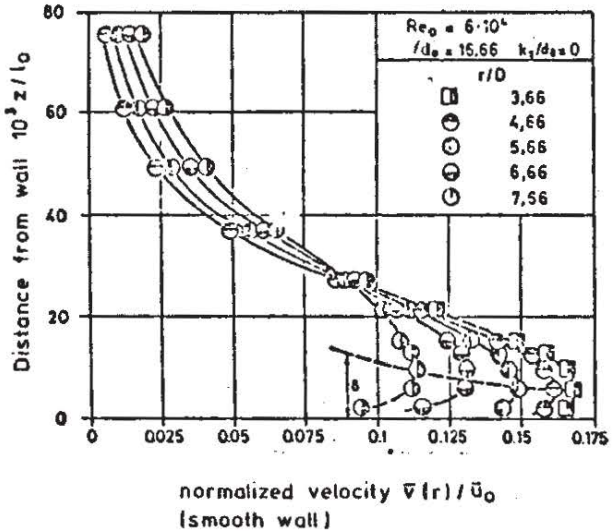

normalized velocity $\bar{v}(r) / \bar{u}_0$
(smooth wall)

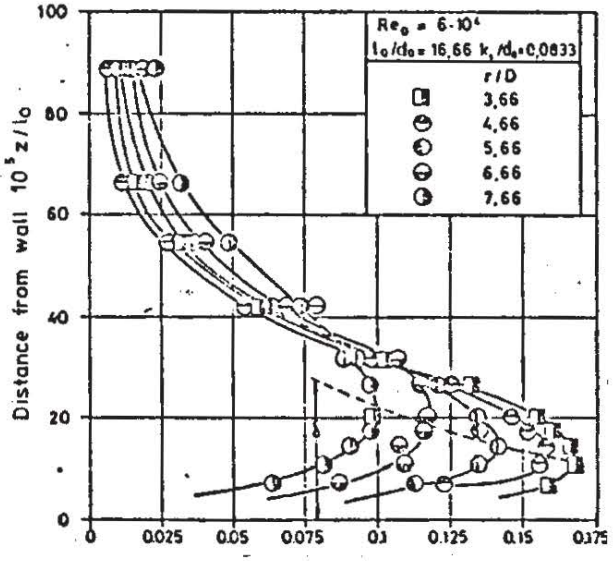

normalized velocity $v(r) / u_0$
(rough wall)

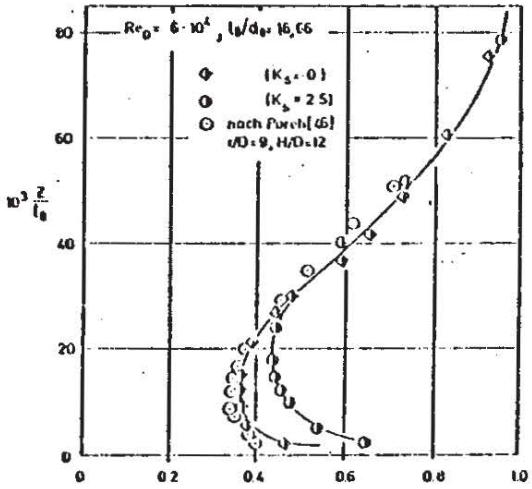

local intensity of radial velocity fluctuations $\sqrt{\overline{v'^2}} / \bar{v}(z)$

SFB 80 B 2	Velocity distribution in the wall jet region	3

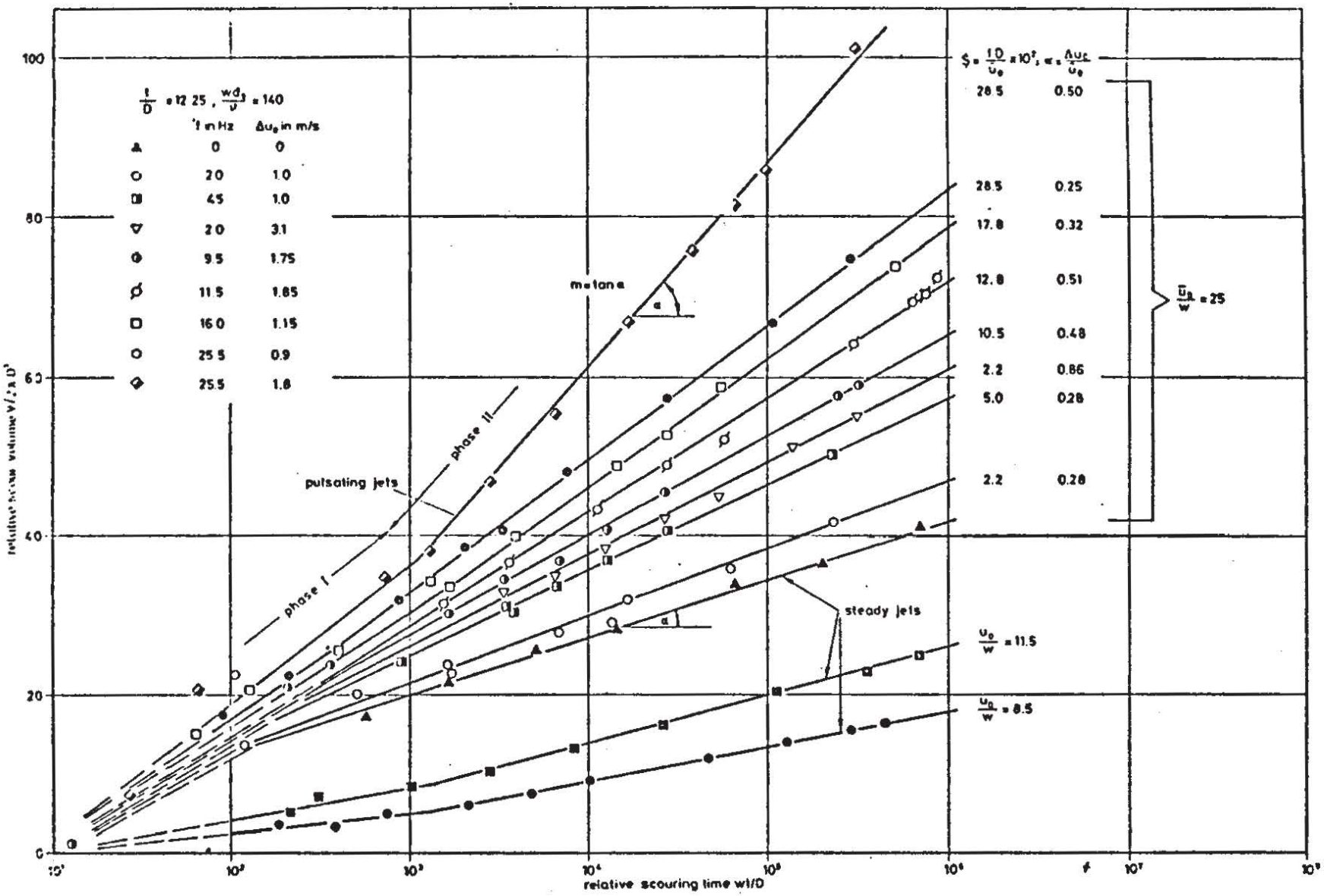

SFB 80 B 2	Time development of scour volume for steady and pulsating jets	4

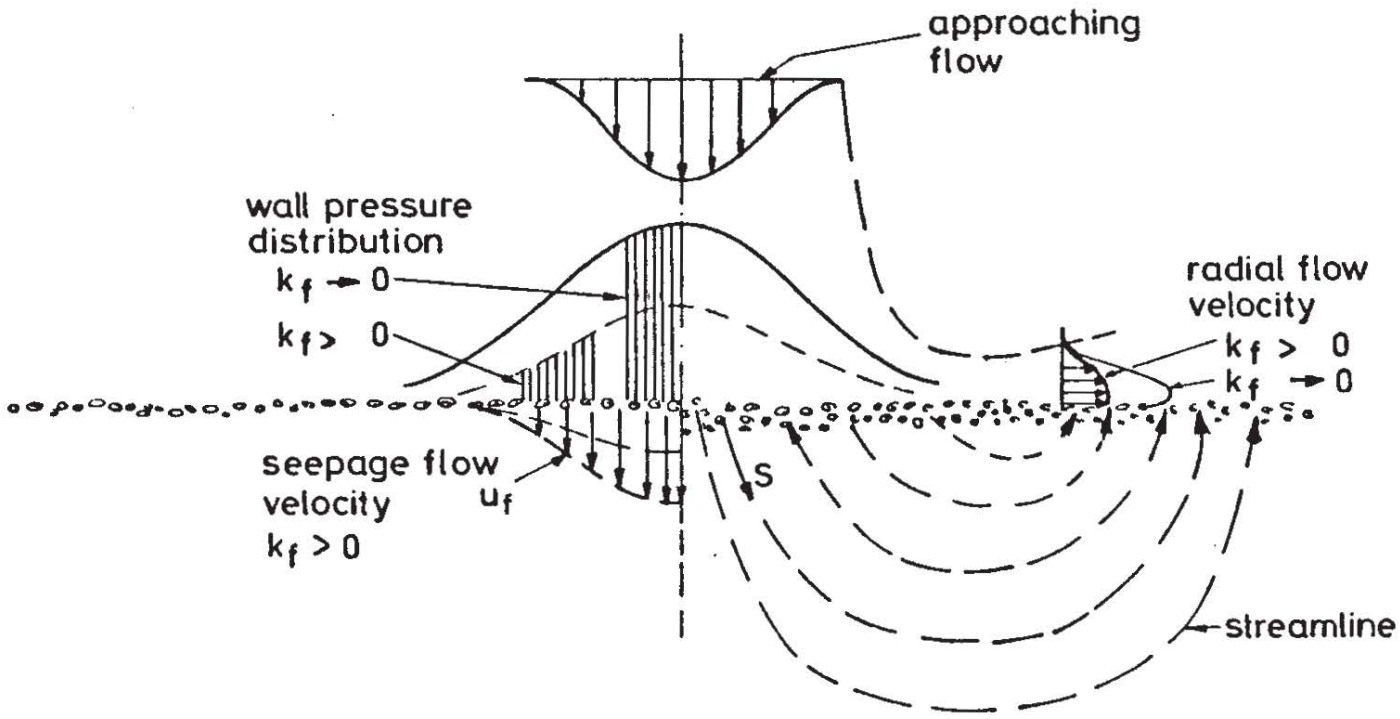

SFB 80 B 2	Influence of seepage flow on the pressure and velocity field at a permeable boundary	5

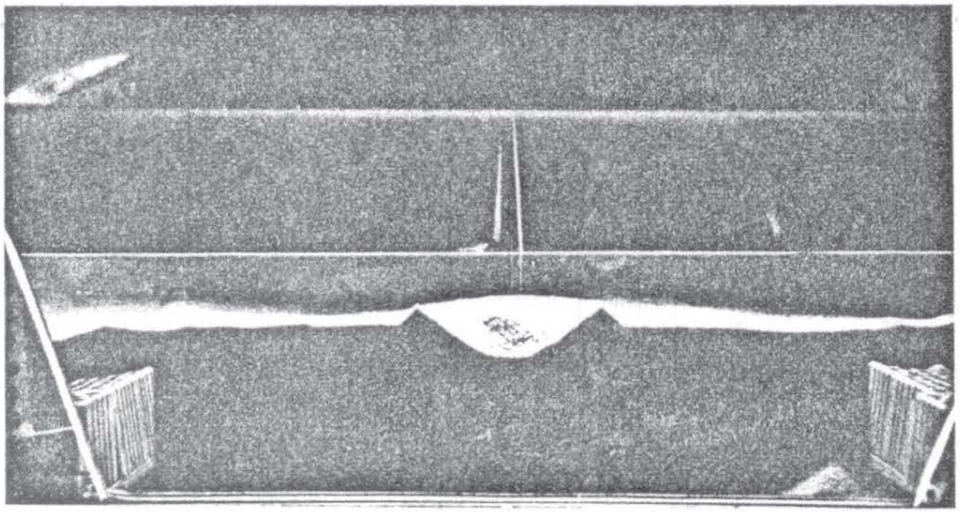

Form I

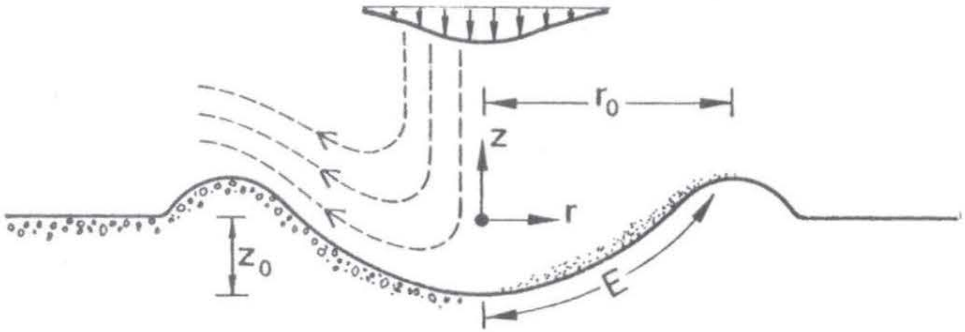

stagnation pressure of the impinging jet

$Re_s = 140 : \quad 1.2 \lesssim \frac{p_s}{\frac{\varrho}{2} w^2} \lesssim 3.0 : \quad \frac{z}{z_0} = \varphi_I \left(\frac{r}{r_0} \right)$

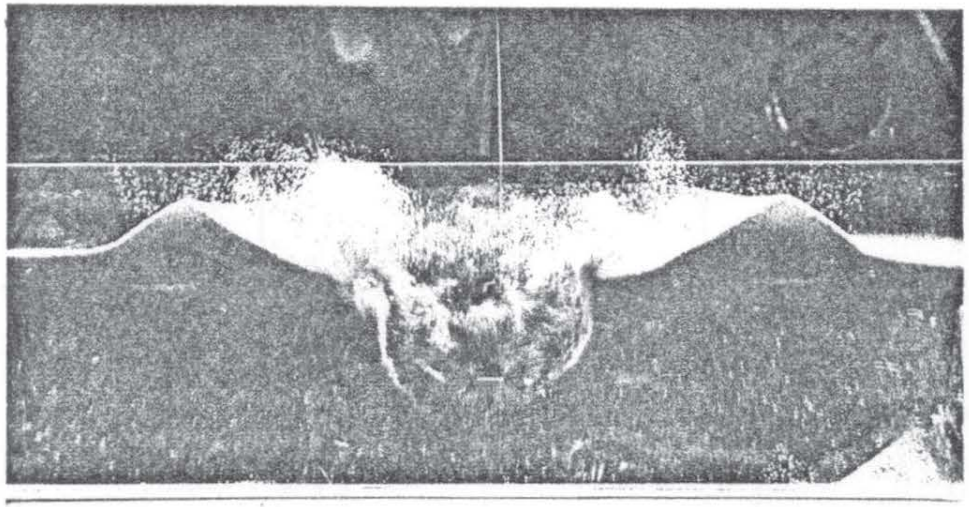

Form II

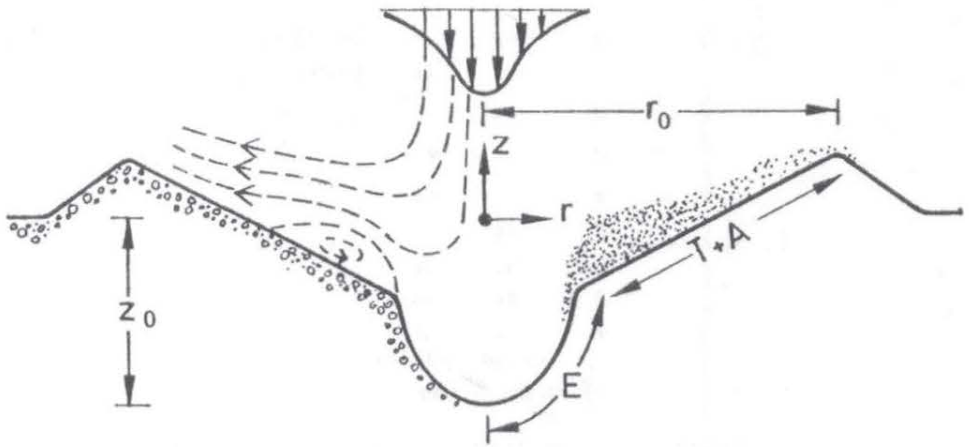

$\frac{p_s}{\frac{\varrho}{2} w^2} \gtrsim 6.5 : \quad \frac{z}{z_0} = \varphi_{II} \left(\frac{r}{r_0}, \frac{p_s}{\frac{\varrho}{2} w^2} \right)$

SFB 80 B 2	Similarity profiles of the scour hole	6

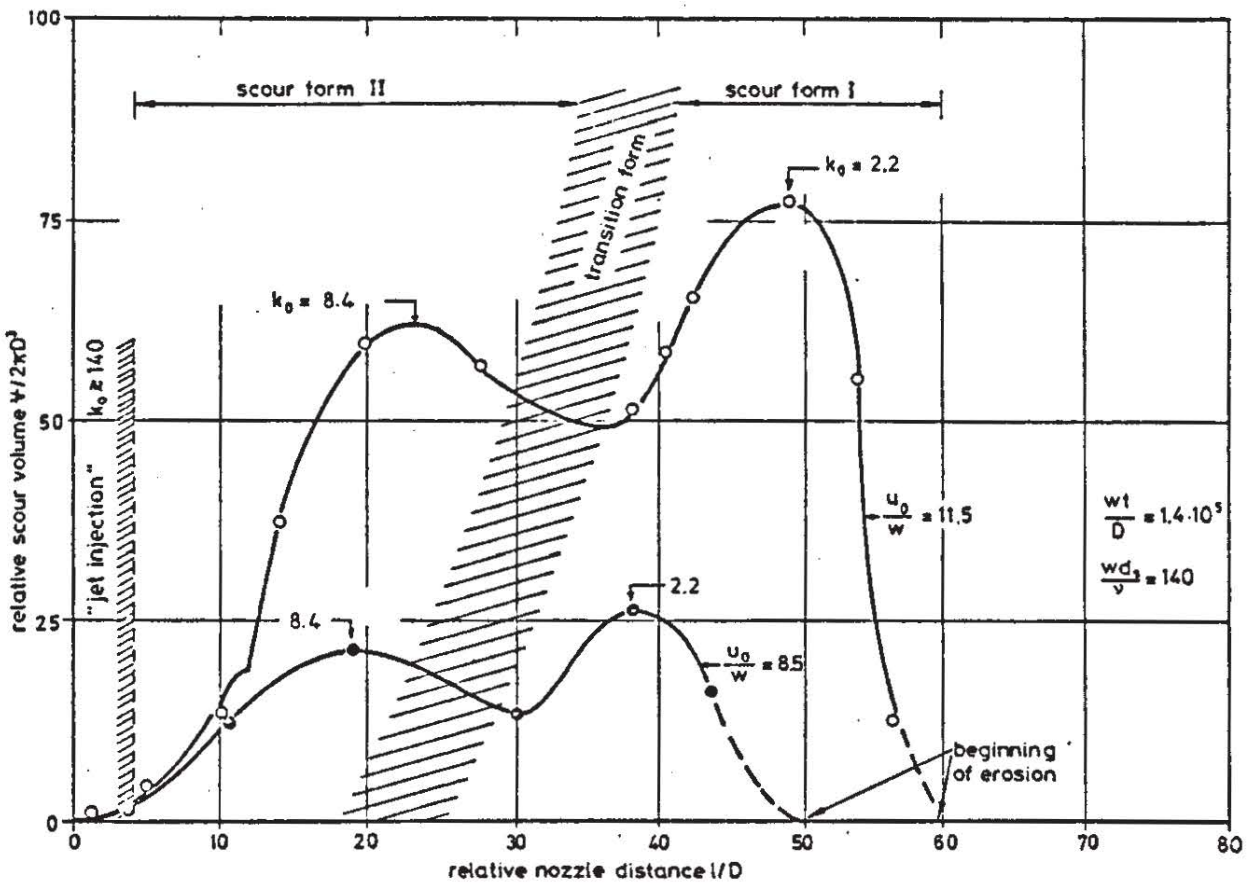

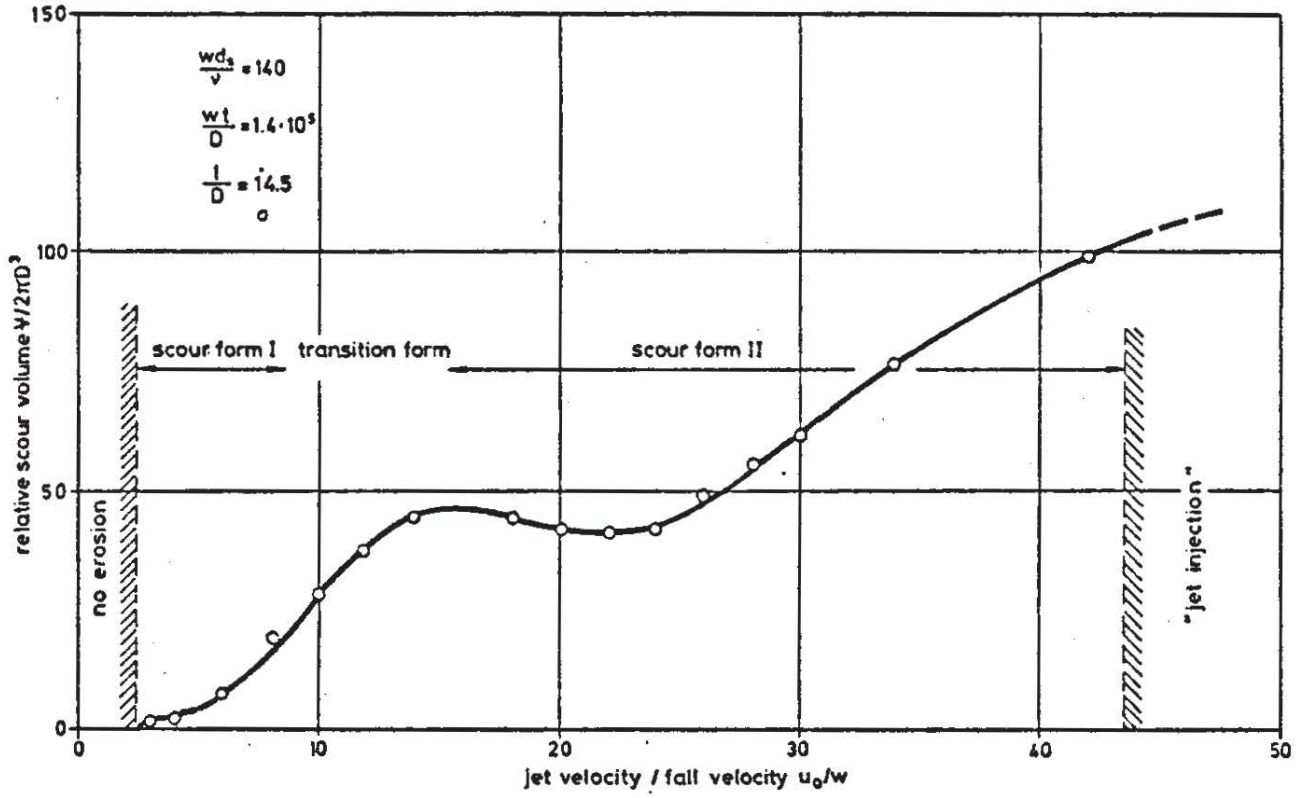

SFB 80 B 2	Effect of nozzle distance and jet velocity on scour volume	7

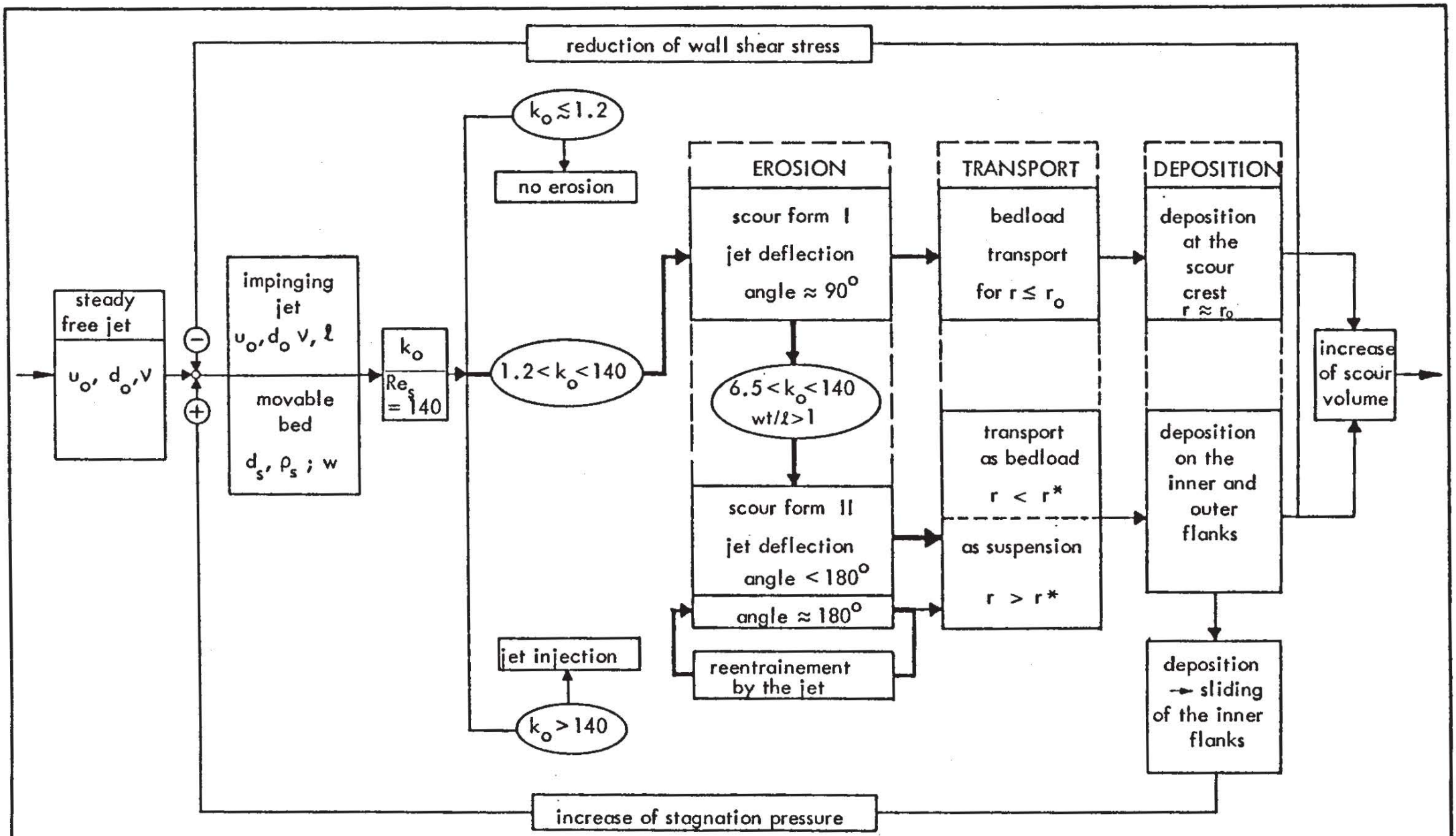

SFB 80 B 2	Block - diagramm of jet - erosion	8

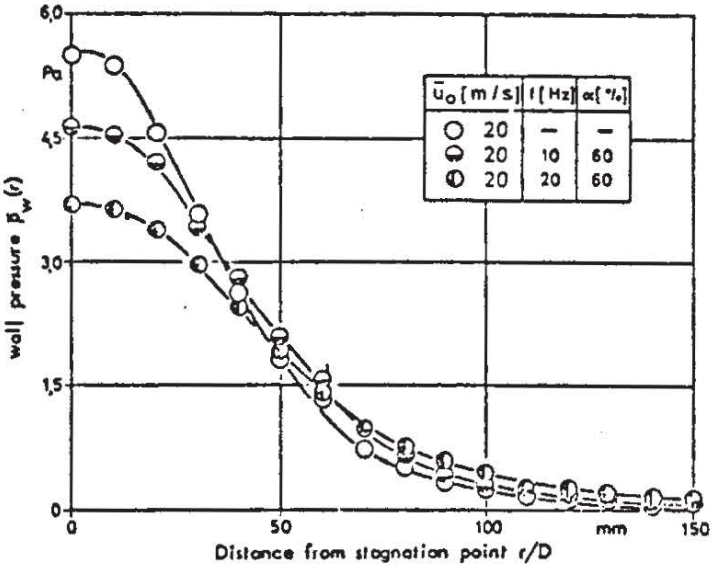

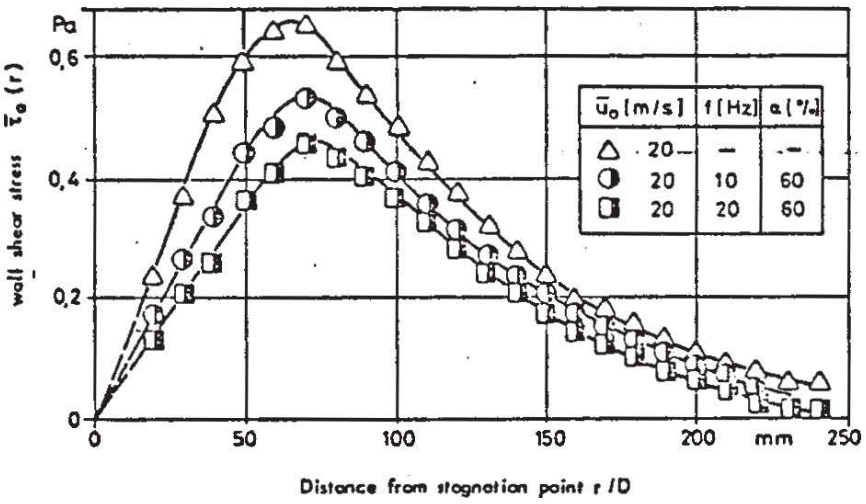

SFB 80 B 2	Influence of pulsation frequency on wall pressure and wall shear stress	9

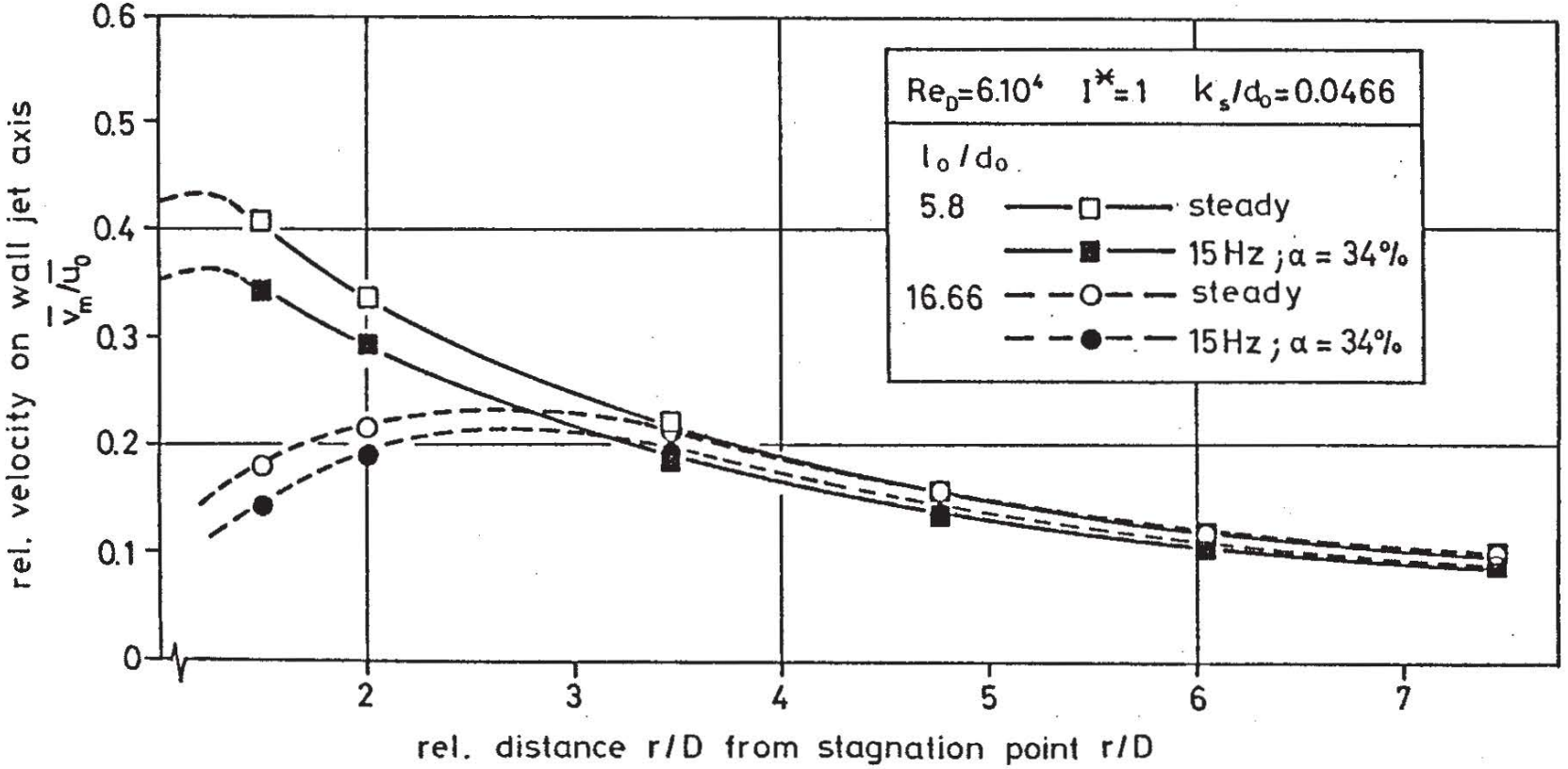

SFB 80 B 2	Developement of max. velocity parallel to the wall on wall jet axis	10

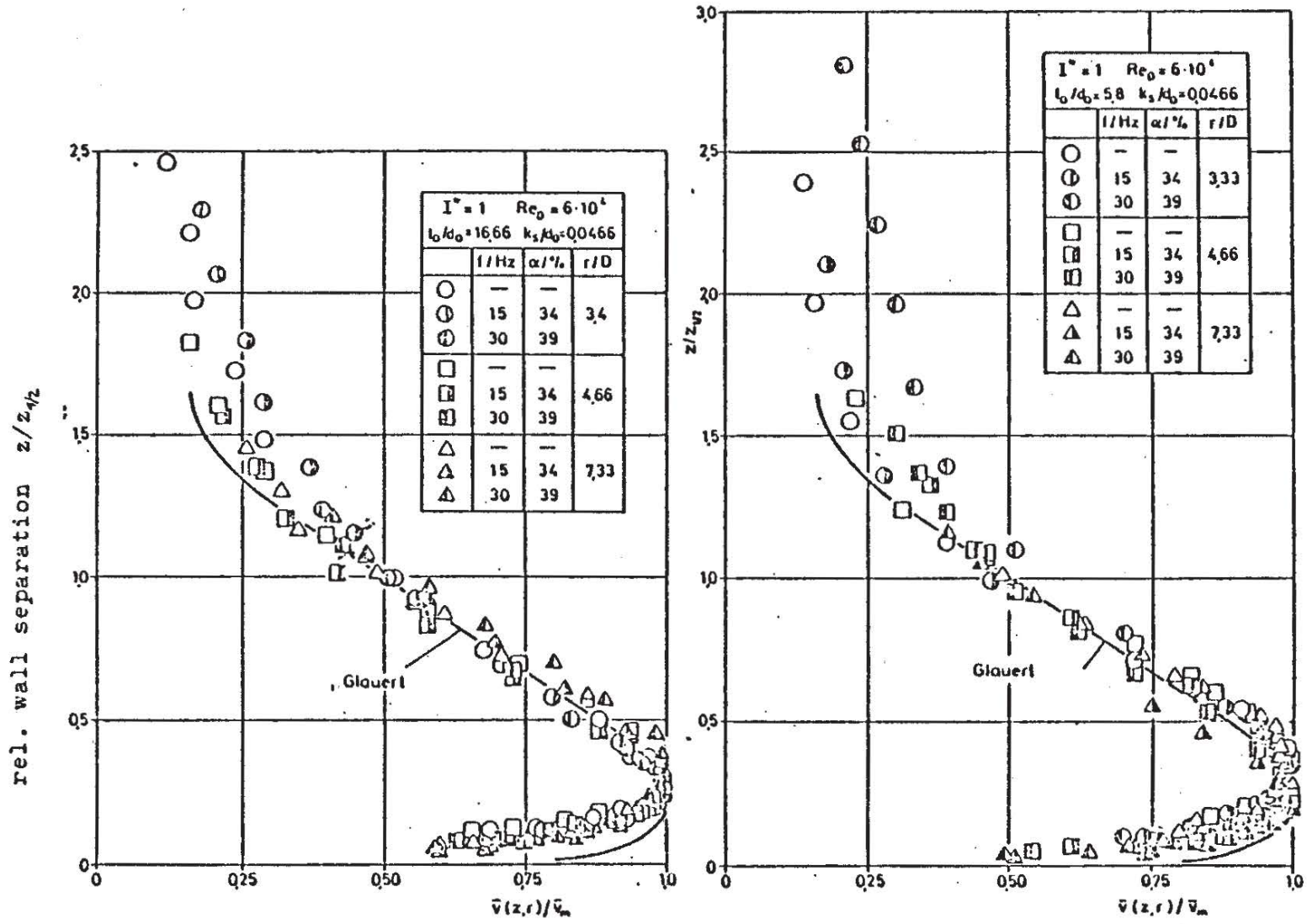

I/Hz	α/%	r/D
—	—	
15	34	3,4
30	39	
—	—	
15	34	4,66
30	39	
—	—	
15	34	7,33
30	39	

$I^* = 1$ $Re_0 = 6 \cdot 10^4$ $l_0/d_0 = 16.66$ $k_s/d_0 = 0.0466$

I/Hz	α/%	r/D
—	—	
15	34	3,33
30	39	
—	—	
15	34	4,66
30	39	
—	—	
15	34	7,33
30	39	

$I^* = 1$ $Re_0 = 6 \cdot 10^4$ $l_0/d_0 = 5.8$ $k_s/d_0 = 0.0466$

(l_0/d_0 = 16.66)

(l_0/d_0 = 5.8)

SFB 80 B 2	Similarity profiles of time averaged velocity within wall jet region	11

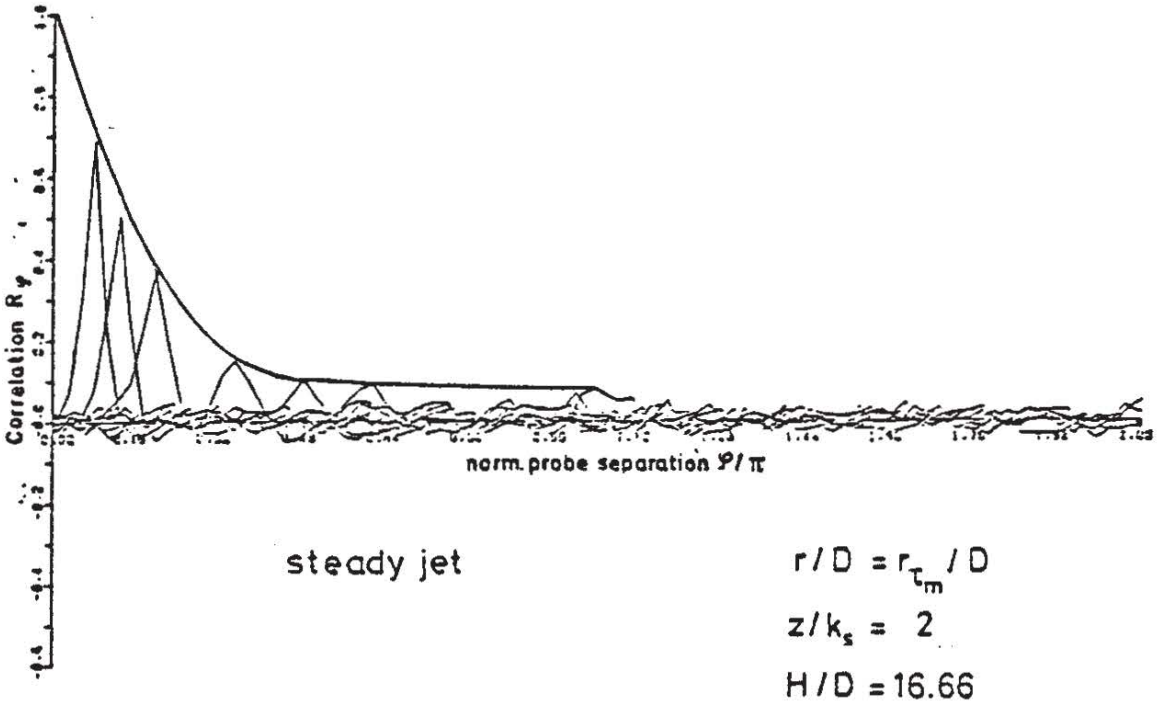

steady jet

$r/D = r_{\tau_m}/D$

$z/k_s = 2$

$H/D = 16.66$

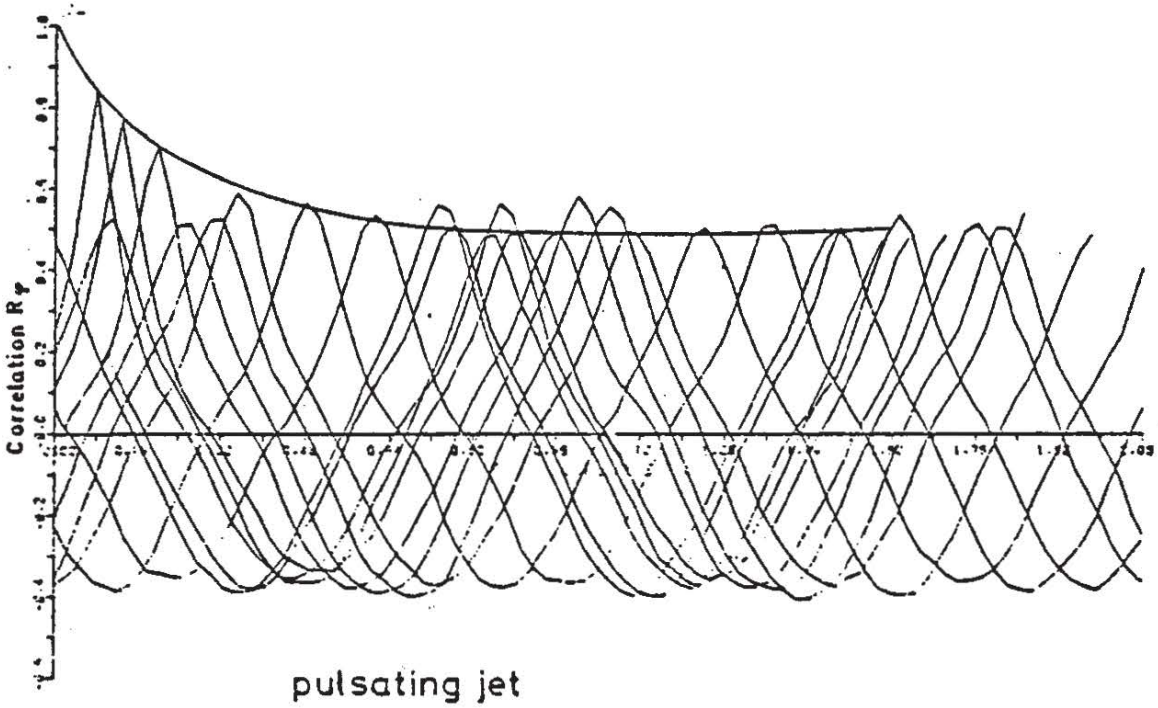

pulsating jet

SFB 80 B 2	Azimuthal crosscorrelation of radial velocity fluctuation without and with pulsation	12

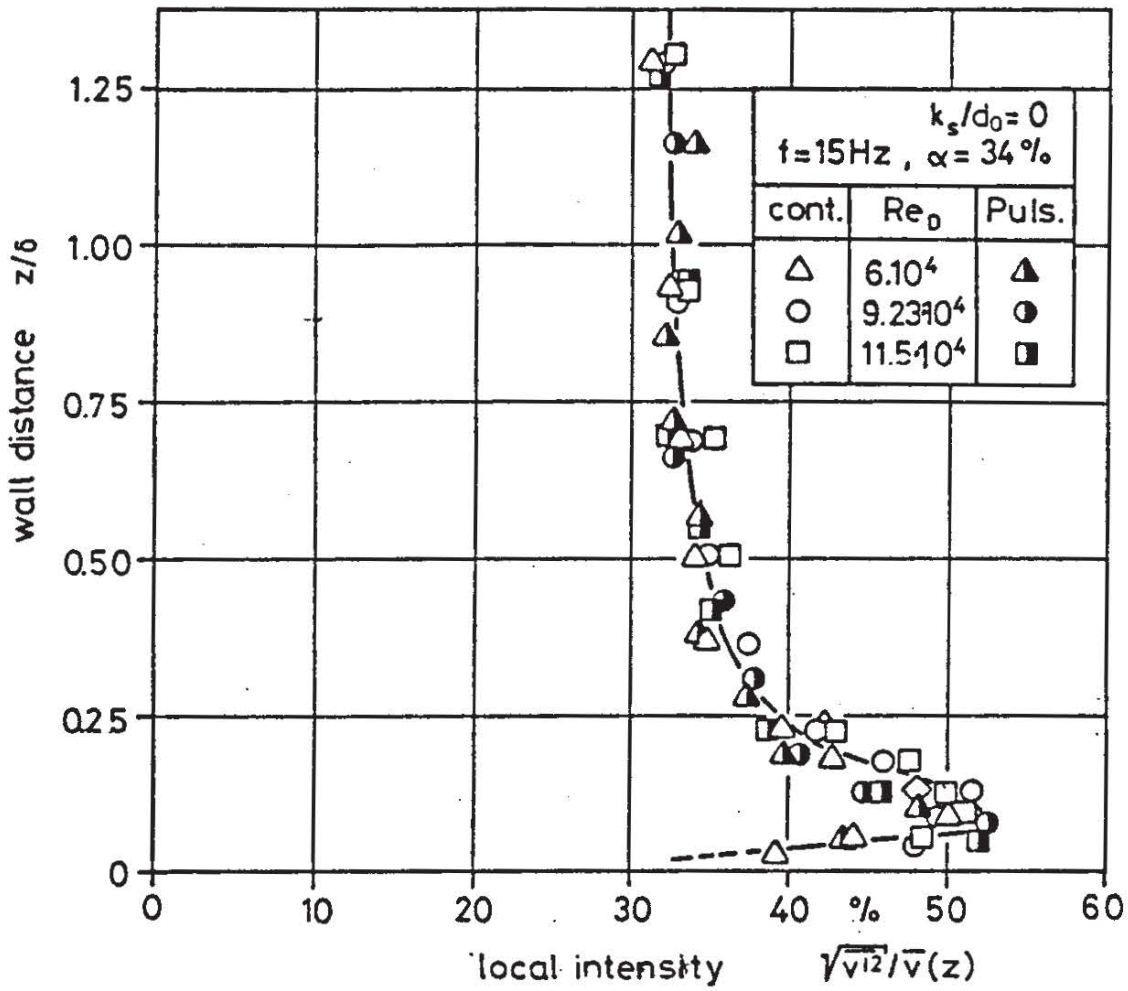
$k_s/d_0 = 0$
f=15Hz , α= 34 %
cont.
Re_D
Puls.
6.10⁴
9.2310⁴
11.5410⁴
wall distance z/δ
1.25
1.00
0.75
0.50
0.25
0
0
10
20
30
40
%
50
60
local intensity $\sqrt{\overline{v'^2}}/\bar{v}(z)$

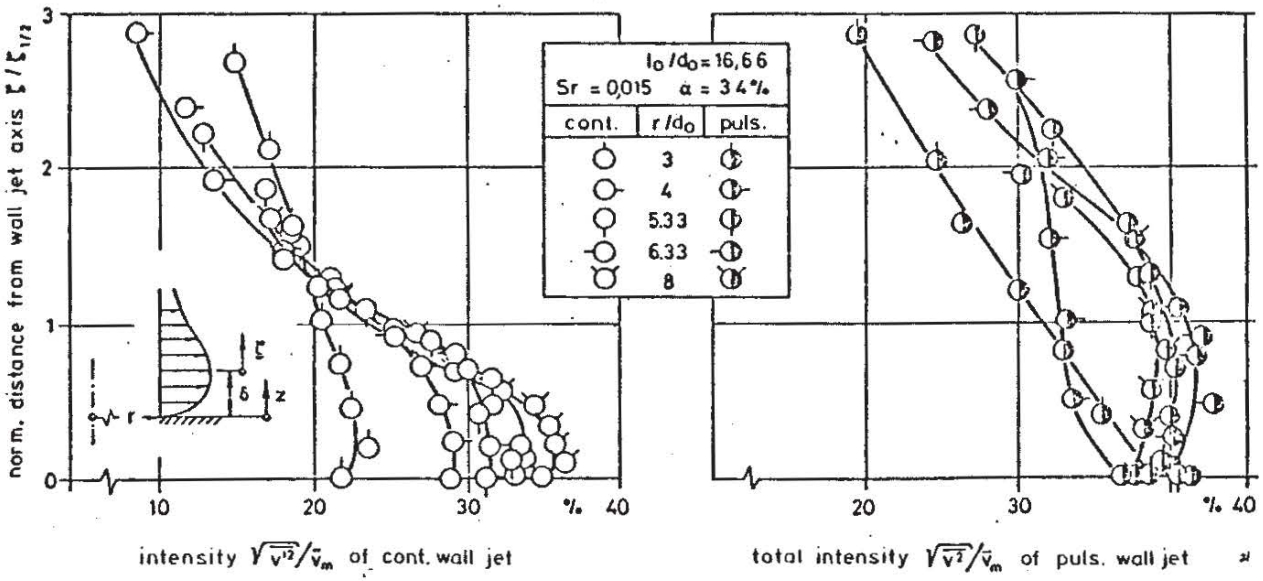

SFB 80 B 2	Comparison of axial fluctuation intensities in the outer shear layer of the wall jet region (l_0/d_0 = 16.66)	14

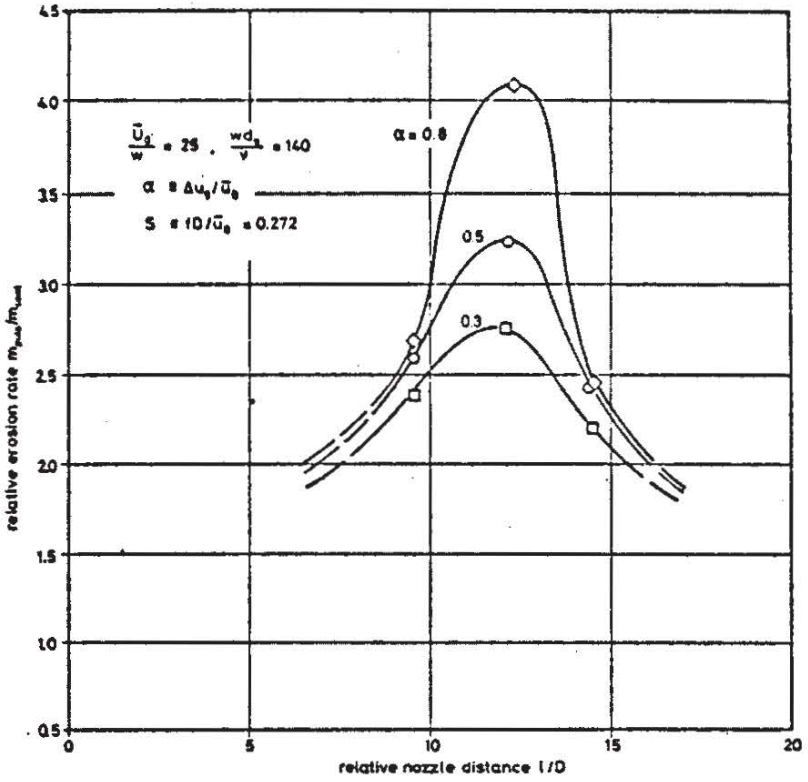

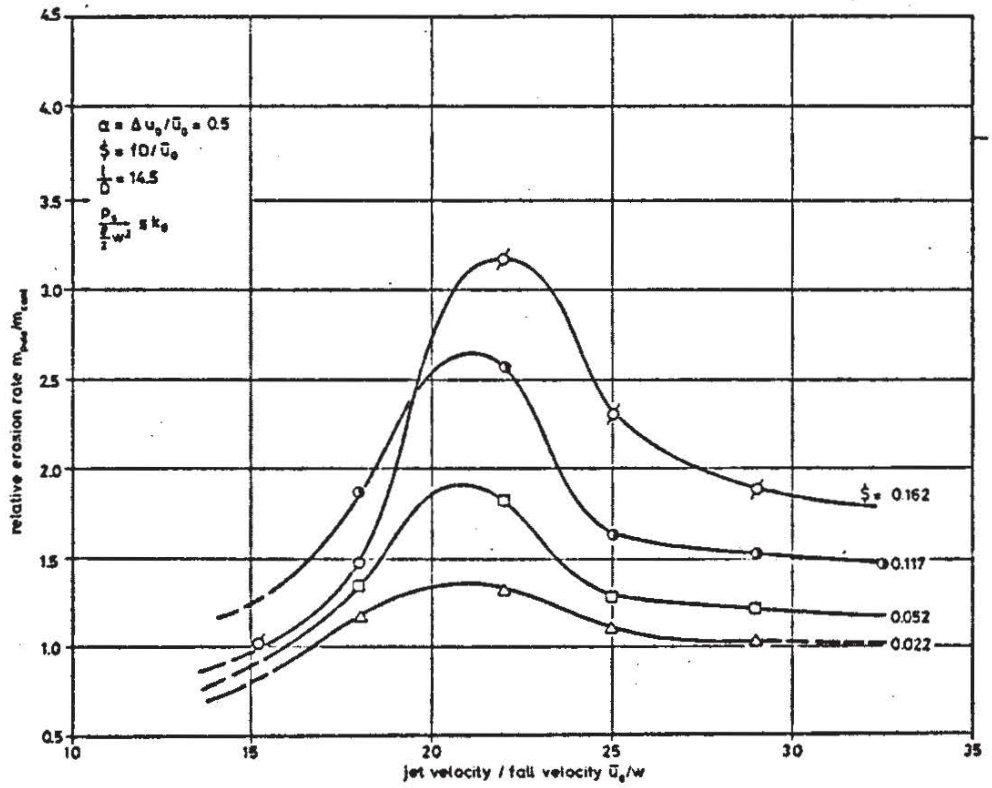

SFB 80 B 2	Effect of amplitude and frequency of the pulsation on the increase of the erosion rate	15

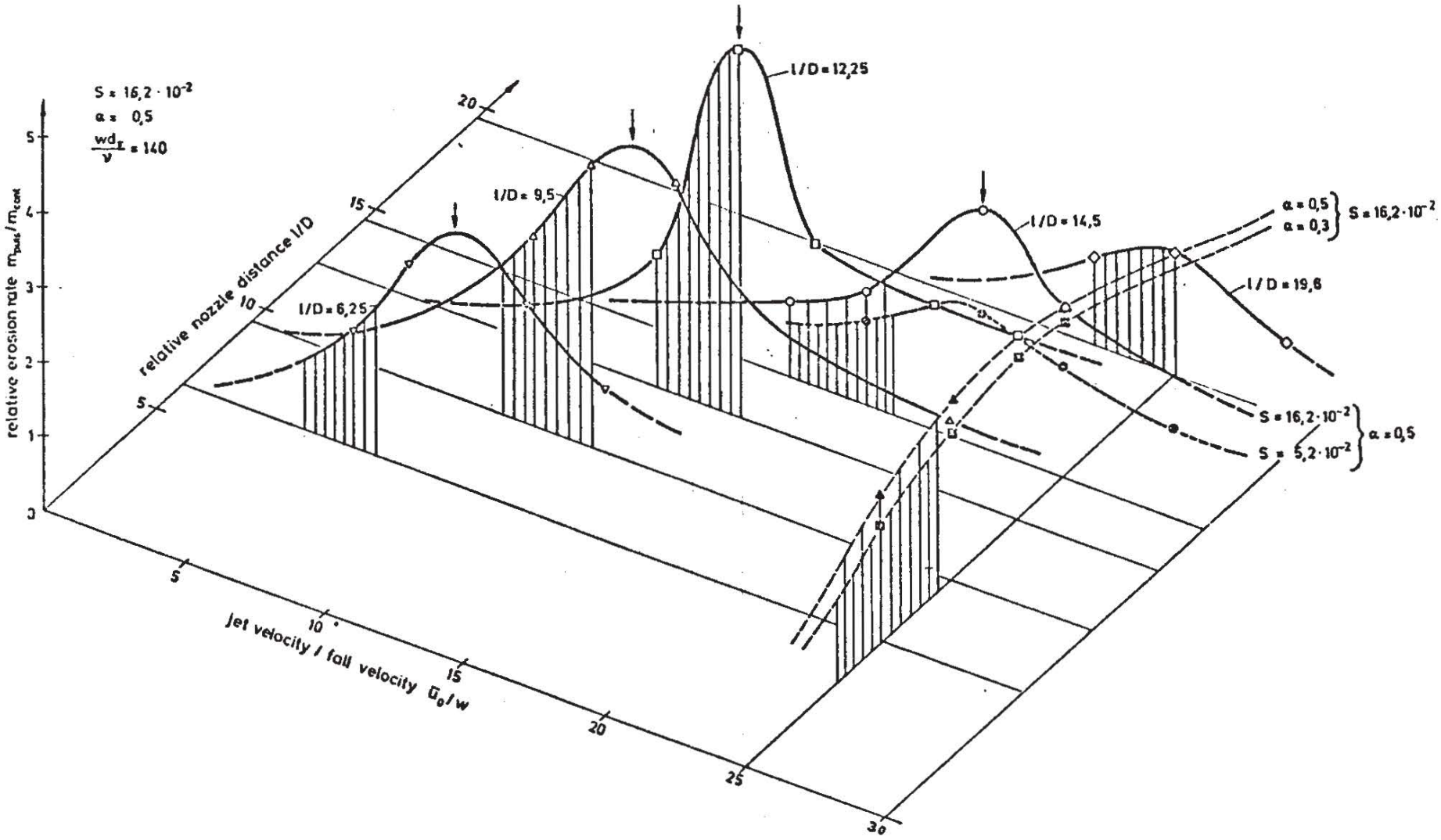

SFB 80 B 2	Increase of erosion rate due to pulsation depending on nozzle distance and jet velocity	16